INVESTIGATION OF EFFECT OF KAOLIN ADDITION ON COMBUSTION CHARACTERISTIC OF OLIVE RESIDUE

A THESIS SUBMITTED TO
THE GRADUATE SCHOOL OF NATURAL AND APPLIED SCIENCES
OF
MIDDLE EAST TECHNICAL UNIVERSITY

BY

ÖZGE BATIR

IN PARTIAL FULFILLMENT OF THE REQUIREMENTS
FOR
THE DEGREE OF MASTER OF SCIENCE
IN
CHEMICAL ENGINEERING

AUGUST 2017

Approval of thesis:

INVESTIGATION OF EFFECT OF KAOLIN ON COMBUSTION CHARACTERISTIC OF OLIVE RESIDUE

submitted by **ÖZGE BATIR** in partial fulfillment of the requirements for the degree of **Master of Science in Chemical Engineering Department, Middle East Technical University** by,

Prof. Dr. Gülbin Dural Ünver
Dean, Graduate School of **Natural and Applied Sciences** _____

Prof. Dr. Halil Kalıpçılar
Head of Department, **Chemical Engineering** _____

Assoc. Prof. Dr. Görkem Külah
Supervisor, **Chemical Engineering Dept., METU** _____

Prof. Dr. Nevin Selçuk
Co-Supervisor, **Chemical Engineering Dept., METU** _____

Examining Committee Members:

Prof. Dr. Murat Köksal
Mechanical Engineering Dept., Hacettepe University _____

Assoc. Prof. Dr. Görkem Külah
Chemical Engineering Dept., METU _____

Assoc. Prof. Dr. Serkan Kıncal
Chemical Engineering Dept., METU _____

Asst. Prof. Dr. Erhan Bat
Chemical Engineering Dept., METU _____

Asst. Prof. Dr. İnci Ayrancı
Chemical Engineering Dept., METU _____

Date: 14.08.2017

I hereby declare that all information in this document has been obtained and presented in accordance with academic rules and ethical conduct. I also declare that, as required by these rules and conduct, I have fully cited and referenced all material and results that are not original to this work.

Name, Last Name: Özge Batır

Signature:

ABSTRACT

INVESTIGATION OF EFFECT OF KAOLIN ADDITION ON COMBUSTION CHARACTERISTIC OF OLIVE RESIDUE

Batır, Özge
M.Sc., Department of Chemical Engineering
Supervisor : Assoc. Prof. Dr. Görkem Külah
Co-Supervisor: Prof. Dr. Nevin Selçuk

August 2017, 69 pages

In this thesis study, effect of kaolin addition on combustion characteristic of olive residue was investigated by using thermogravimetric analyzer (TGA) combined with Fourier-transform infrared (FTIR) spectrometer in parallel with ash characteristics by X-Ray Fluorescence (XRF) and X-Ray Diffraction (XRD). The experiments were carried out by burning olive residue with 2%, 4% and 8% by wt. kaolin at 900˚C. Results reveal that addition of kaolin leads to decrease in rate of weight loss during char combustion and hence increase in CO emission due to decrease in burning quality caused by dilution effect of kaolin in the mixture. Increase in HCl(g) and SO_2(g) concentrations with kaolin addition observed in FTIR results evaluated together with XRF and XRD results demonstrated the pathway of reactions for the capture of potassium by kaolin and formation of high melting temperature kalsilite crystals. Potassium retention in ash was found to increase up to 4% kaolin addition; however, no significant improvement in potassium retention was observed with further addition of kaolin due to abundant amount of Al and Si introduced via kaolin. Moreover, ash melting temperature was found to increase by 200˚C with the addition of 4% kaolin

during ash fusion tests. The results showed that optimum 4% kaolin addition decreases slagging and fouling tendency of olive residue during combustion.

Keywords: Additive, kaolin, biomass, olive residue, combustion

ÖZ

KAOLİN EKLENMESİNİN PRİNANIN YANMA KARAKTERİSTİĞİNE ETKİSİNİN İNCELENMESİ

Batır, Özge

Yüksek Lisans, Kimya Mühendisliği Bölümü
Tez Yöneticisi : Doç. Dr. Görkem Külah
Ortak Tez Yöneticisi: Prof. Dr. Nevin Selçuk

Ağustos 2017, 69 sayfa

Bu tez çalışmasında, kaolin eklenmesinin prinanın yanma karakteristiğine olan etkisi termogravimetrik analiz yöntemi (TGA) ve buna bağlı olan Fourier dönüşümü kızılötesi spektrometresi (FTIR) kullanılarak; aynı zamanda kül karakteristiğine olan etkisi X-Işını Floresans Spektometresi (XRF) ve X-Işını Difraktometresi (XRD) kullanılarak incelenmiştir. Deneyler prina ve prina ile kütlece %2, %4 ve %8 kaolin karışımlarının 900°C'de yakılmasıyla yürütülmüştür. Deneysel sonuçlar, kaolin eklenmesinin kokun yanması sırasındaki kütle kaybı oranını düşürdüğünü, bunun sonucunda CO emisyonunu arttırdığını, bunun da kaolinin karışımda seyreltme etkisi yapmasıyla yanma kalitesinin azalması olduğunu göstermektedir. FTIR sonuçlarında gözlemlenen HCl(g) ve SO_2(g) konsantrasyonlarının kaolin eklenmesiyle artışının XRF ve XRD sonuçlarıyla birlikte değerlendirilmesi, kaolinin potasyumu tutması için izlenen reaksiyon yolunu ve yüksek erime sıcaklığına sahip kalsilit kristalinin oluşumunu açıklamıştır. Külde tutulan potasyumun, %4 kaolin eklenmesine kadar arttığı bulunmuş, ancak daha yüksek miktarda kaolin eklenmesi ile kaolin tarafından

çok miktarda Al ve Si'nin sisteme sokulmasından dolayı potasyum tutulmasında önemli bir ilerleme gözlenmemiştir. Buna ek olarak, %4 kaolin eklenmesi ile kül ergime sıcaklığında 200°C artış olduğu görülmüştür. Sonuçlar göstermektedir ki, optimal %4 kaolin eklenmesi prinanın yanma sırasında kirlenme ve curuf oluşturma eğilimini azaltmaktadır.

Anahtar kelimeler: Katkı maddesi, kaolin, biyokütle, prina, yanma

To my great family…

ACKNOWLEDGEMENTS

I wish to express my deepest gratitude to my co-supervisor, Prof. Dr. Nevin Selçuk for her guidance, advice, patience and encouragement throughout the development of this study. I would like to show my appreciation to my supervisor Assoc. Prof. Dr. Görkem Külah, for her valuable suggestions, support and utmost contributions to the study.

Financial supports provided by Middle East Technical University (METU) through BAP-07-02-2017-004-197 project is gratefully acknowledged. I would like to thank to Prof. Dr. Necati Özkan and Aysun Güney for TGA-FTIR analyses, Aydın Köse from NORMLAB and Leyla Molu for the fuel analyses and Serkan Yılmaz for SEM-EDX analyses.

Many thanks to my sisters from another mother, Aybüke Karakaş, Ceren Karataş and Özge Meriç Demir for their precious friendship and support. I also would like to thank to my master girls, Merve Sarıyer and Özge Şen; my dearest roommates Berrak Erkmen and Gülbin Tanrıseven; Merve Özkutlu, Fatma Şahin, Cihan Ateş and all my other friends that I am not able to mention in a page of acknowledgement for their supports and hopeful point of view in all situations.

Last but not least, I want to express my deepest pleasure to my mother Leyla Batır, father Lütfü Batır and my little sister Neris Batır for their unconditional love, sacrifices, unshakable faith in me, and endless support over my whole life. They are my luck. Without them, I cannot be the person I am right now.

TABLE OF CONTENTS

ABSTRACT v

ÖZ vii

ACKNOWLEDGEMENTS x

TABLE OF CONTENTS xi

LIST OF TABLES xiii

LIST OF FIGURES xiv

CHAPTERS

1. INTRODUCTION 1

1.1. General 1

1.2. Aim and Scope of the Thesis 3

2. ASH RELATED ISSUES IN BIOMASS COMBUSTION 5

2.1. Operational Problems Associated with Biomass Ash 7

3. EFFECT OF KAOLIN ADDITION ON ALLEVIATION OF ASH RELATED PROBLEMS 13

3.1. Pathway of Potassium during Biomass Combustion and its Capture by Kaolin Addition 13

3.2. Literature Review on Combustion Studies of Biomass with Kaolin Addition 16

4. EXPERIMENTAL 23

4.1. General 23

4.2. Materials 23

4.3. Experimental Method 25
4.3.1. TGA-FTIR Analyses 25
4.3.2. Sintering Tests 27
4.3.3. XRF and XRD Analysis 27
4.3.4. SEM-EDX Analysis 28
5. RESULTS AND DISCUSSIONS 29
5.1. General 29
5.2. TGA-FTIR Analyses of Combustion of Olive Residue and Olive Residue-Kaolin Mixtures 29
5.3. Sintering Tests 37
5.4. XRF Analyses of Ashes of Olive Residue and Olive Residue-Kaolin Mixtures 40
5.4.1. Predicting Ash Melting Temperature from Ternary Phase Diagram ... 43
5.5. Determination of Ash Fusion Temperatures 46
5.6. XRD Analysis of Ashes of Olive Residue and Olive Residue-Kaolin Mixtures 47
6. CONCLUSIONS 51
6.1. General 51
6.2. Suggestions for Future Work 52
REFERENCES 53
APPENDICES ..... **Error! Bookmark not defined.**

LIST OF TABLES

TABLES

Table 2.1 Proximate and ultimate analyses of biomass and coal [29] 6
Table 4.1 Characteristics and ash analysis of olive residue 24
Table 4.2 Chemical composition of Kaolin 190 (%) 25
Table 5.1 Combustion characteristics of olive residue (OR) and olive residue-kaolin mixtures 31
Table 5.2 XRF analysis results of ashes of olive residue (OR) and olive residue-kaolin mixtures 41
Table 5.3 Content of olive residue ash and olive residue ash in kaolin mixtures 42
Table 5.4 Base to acid ratio and alkali indices of ashes of olive residue (OR) and olive residue-kaolin mixtures 43
Table 5.5 Relative amount of K_2O, SiO_2 and Al_2O_3 in the ashes of olive residue (OR) and olive residue-kaolin mixtures 44
Table 5.6 Predicted initial deformation temperature (IT) interval of olive residue and olive-residue kaolin mixtures 45
Table 5.7 Ash fusion temperatures of olive residue (OR) and olive residue + 4% kaolin mixture 47

LIST OF FIGURES

FIGURES

Figure 1.1 Share of total primary energy supply in world in year 2014 [3]..... 1
Figure 1.2 World electricity generation by fuel, (2012-2040) [4] 2
Figure 2.1 Biomass ash compositions [29] 7
Figure 2.2 Schematic of the formation processes of the main ash-related issues in biomass combustion [33] 8
Figure 4.1 Photograph of olive residue and kaolin additive 23
Figure 4.2 Schematic diagram of TGA-FTIR system [83] 26
Figure 5.1 TGA (a) and DTG (b) profiles of combustion of olive residue (OR) and olive residue-kaolin (K) mixtures 30
Figure 5.2 Evolved gas formation profiles of olive residue (OR) and olive residue-kaolin (K) mixtures during combustion tests 35
Figure 5.3 Pathway of potassium during combustion of olive residue with and without kaolin addition [15,33,46,47,53,56,58,62] 37
Figure 5.4 Photographs of olive residue ash 38
Figure 5.5 Photographs of olive residue + 2% kaolin mixture ash 39
Figure 5.6 Photographs of ashes of olive residue (a), olive residue + 2% (b), 4% (c), 8% (d) kaolin mixtures after sintering tests 40
Figure 5.7 Potassium retention within the ash with and without kaolin addition 42
Figure 5.8 K_2O-SiO_2-Al_2O_3 ternary phase diagram [66]..... 45
Figure 5.9 Picture of olive residue ash sample during ash fusion test 46
Figure 5.10 Picture of olive residue + 4% kaolin mixture ash sample during ash fusion test 46
Figure 5.11 XRD pattern of kaolin..... 48

Figure 5.12 XRD pattern of olive residue olive residue-kaolin mixture ashes 49
Figure A.1 SEM images of olive residue ash 64
Figure A.2 EDX area analysis of large olive residue ash 64
Figure A.3 EDX area analysis of fine olive residue ash samples 65
Figure A.4 SEM images of olive residue + 2% kaolin mixture ash (a: overall image, b: large ash particle, c: fine ash particle) 66
Figure A.5 EDX area analysis of large olive residue + 2% kaolin mixture ash 66
Figure A.6 EDX area analysis of fine olive residue + 2% kaolin mixture ash 67
Figure A.7 SEM images of olive residue + 8% kaolin mixture ash (a: overall image, b: overall fine particles, c: large ash particle, d: fine ash particle) 68
Figure A.8 EDX area analysis of large olive residue + 8% kaolin mixture ash 68
Figure A.9 EDX area analysis of fine olive residue + 8% kaolin mixture ash 69
Figure A.10 Average EDX analysis results of ashes of olive residue and olive residue-kaolin mixtures 69

CHAPTER 1

INTRODUCTION

1.1. General

The demand for electric power continues to rise due to population growth, technological and economical development. Coal is predicted to be the dominant fossil fuel for energy production for decades with progressively improving clean coal technologies and 891 billion tons of proved reserves [1]. Gradual introduction of increasingly restrictive legislations on emissions from combustion sources has been increasing the interest in biomass combustion. Biomass is a renewable energy source due to the fact that it is considered as CO_2-neutral fuel and contributes to the reduction in pollutant emissions [2]. As illustrated in Figure 1.1, biomass is the fourth largest energy source after oil, coal and gas and that about 10 % of world's energy is produced from biomass.

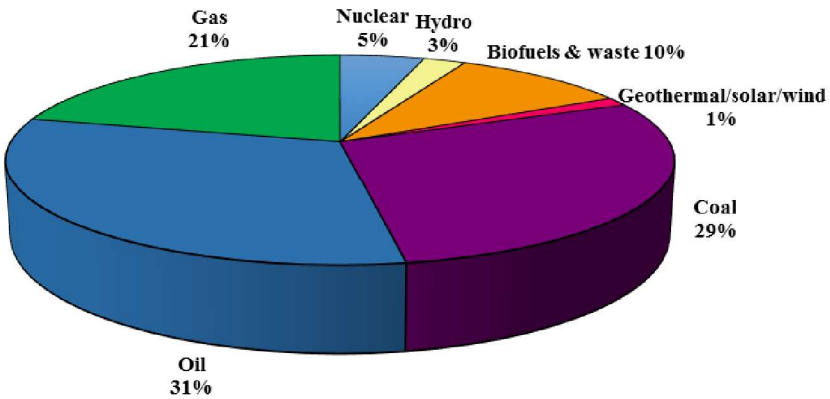

Figure 1.1 Share of total primary energy supply in world in year 2014 [3].

The share of biomass is expected to rise in the following years due to increasingly strict legislations on emissions from fossil fuel sources. The projections on electricity generation till year 2040 given in Figure 1.2 also show the increase in electricity production from renewable sources.

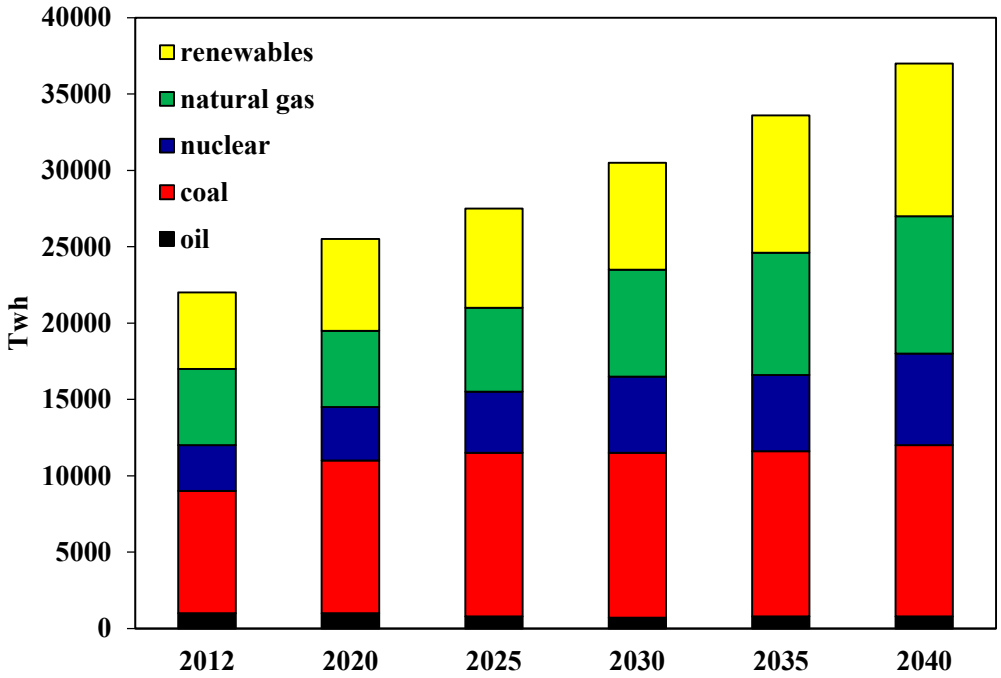

Figure 1.2 World electricity generation by fuel, (2012-2040) [4]

However, biomass combustion brings some operational problems when burned alone. The most common problems encountered in industry and utility boilers are severe fouling, slagging and corrosion which are mainly originated from high alkali content of biomass ash [5]. Ash deposits formed on heat transfer surfaces deteriorate heat transfer and lead to loss in thermal efficiency and corrosion [6].

Fluidized bed combustors are preferred in biomass combustion due to their low operation temperature (around 850˚C) which reduces occurrence of ash melting problems. [5]. However, studies on fluidized bed combustion of biomass fuels in beds of sand reveals that single firing of biomass results in low combustion efficiencies and

is still problematic due to operational problems caused by high potassium content of the ash [7-13]. These operational problems can be alleviated by leaching, co-firing of biomass with coal and by addition of additives [14-17]. The first alternative is not economically feasible [18]. Co-firing of biomass with coal has been found to be the most promising alternative; however, it may not be feasible when biomass source and coal mine does not co-exist in the same location [19]. Using additive is an alternative way to prevent operational problems during biomass combustion processes since their usage is eco-friendly, easy to apply and does not require extra maintenance cost for the process [15,20,21]. Additives refer to a group of minerals or products that can alter the ash chemistry, convert problematic species to less troublesome forms and increase the ash melting temperature in thermal processes [16]. In previous studies, various kinds of mineral based additives were used to prevent ash sintering problems like kaolin, calcite, lime, alumina, limestone, silica, dolomite and bentonite [16,22-24]. According to these studies, kaolin, which is an alumina based additive, was shown to increase ash melting temperature of biomass and was verified to be one of the most effective additive [24,25].

1.2. Aim and Scope of the Thesis

Olive residue is a type of biomass obtained during olive oil production process. It is the remaining part of olives after pressing and extraction of olive oil. Turkey is one of the main olive producers with 826 000 ha of olive groves and 1 768 000 tons of annual production [26]. However, olive residue has high concentrations of potassium which results in operational problems like fouling and slagging during its combustion [16, 22, 25, 27]. These problems can be alleviated by addition of kaolin to the system during its combustion. However, before adding kaolin to fluidized bed combustors (FBC), effect of kaolin on combustion characteristic of olive residue needs to be determined by using non-isothermal thermo-gravimetric analysis (TGA) technique which is an inexpensive and simple method that has been used widely in studying the combustion characteristics of fuels.

Absence of studies on the investigation of effect of kaolin on combustion characteristics of olive residue by TGA-FTIR analysis on one hand and the recent trend on utilization of biomass with local reserves in industry and utility boilers on the other necessitate investigation of effect of kaolin addition on combustion characteristics of olive residue. In an attempt to achieve this objective, in this study, TGA-FTIR combustion analysis and quantitative and qualitative analysis of ashes of olive residue and olive residue-kaolin mixtures have been carried out by XRF, XRD and SEM-EDX analyses.

CHAPTER 2

ASH RELATED ISSUES IN BIOMASS COMBUSTION

Biomass describes carbonaceous materials derived from plants. Biomass fuels can be classified as agricultural residues, woody residues, dedicated energy crops and industrial and municipal waste of plant origin [28]. Table 2.1 displays proximate and ultimate analyses of some selected biomass and coal. As can be seen from the table, biomass fuels are mainly characterized by their high volatile matter and low ash contents.

Ash compositions of some selected biomass and coal are depicted in Figure 2.1. As can be seen from the figure, biomass ashes have higher portions of alkalis, potassium and sodium, compared to those of coals which leads to lower ash fusion temperature of biomass [29].

High alkali content can cause bed agglomeration, slagging and fouling of heat transfer surfaces which lead to reduced reliability of electricity production from biomass. The successful design and operation of a fluidized bed combustor depends on the ability to control and mitigate these ash related problems [30].

Table 2.1 Proximate and ultimate analyses of biomass and coal [29]

Fuel	**Proximate Analysis (as received, wt %)**				**Ultimate Analysis (dry, wt %)**							
Biomass	Moisture	VM	FC	Ash	C	H	N	S	O	Cl	Ash	LHV (MJ/kg)
Olive residue	8.93	65.30	18.49	7.28	51.70	5.80	1.38	0.30	32.81	0.01	8.00	19.50
Wheat Straw	7.75	72.05	14.46	5.74	46.95	5.36	0.50	0.22	39.70	1.05	6.22	17.23
Rice Straw	11.40	43.41	25.17	20.02	36.90	4.70	0.30	0.06	35.36	0.08	22.60	11.70
Rice husk	11.00	58.00	18.01	12.99	38.42	5.46	0.36	0.04	41.12	0.00	14.60	12.34
Bagasse	5.00	65.54	28.22	1.24	48.58	5.97	0.20	0.05	43.85	0.05	1.30	17.70
Cotton seed cake	6.10	78.70	10.30	4.90	49.29	5.59	1.23	0.00	38.67	0.00	5.22	17.99
Hazelnut shell	12.45	62.70	24.08	0.77	46.76	5.76	0.22	0.67	45.71	0.00	0.88	15.95
Bark	12.00	68.73	15.05	4.22	47.40	5.50	0.30	0.00	42.00	0.00	4.80	17.30
Wood chips	34.90	51.60	13.30	0.20	47.30	6.10	0.20	0.10	46.00	0.00	0.30	11.70
Sawdust	53.30	39.69	6.76	0.15	52.10	6.00	0.10	0.10	41.38	0.002	0.32	7.99
Pine seed shell	13.00	59.60	26.60	0.80	48.50	6.10	0.20	0.10	44.18	0.00	0.92	15.20
Coal												
Bituminous coal	5.49	25.16	52.24	17.11	67.87	3.73	1.34	0.71	8.25	0.00	18.10	25.59
South African coal	2.30	23.00	60.20	14.50	67.20	3.70	1.20	0.60	12.50	0.00	14.80	25.40
Lignite	13.70	32.70	17.20	36.40	38.10	3.20	1.40	2.70	12.40	0.00	42.20	12.26

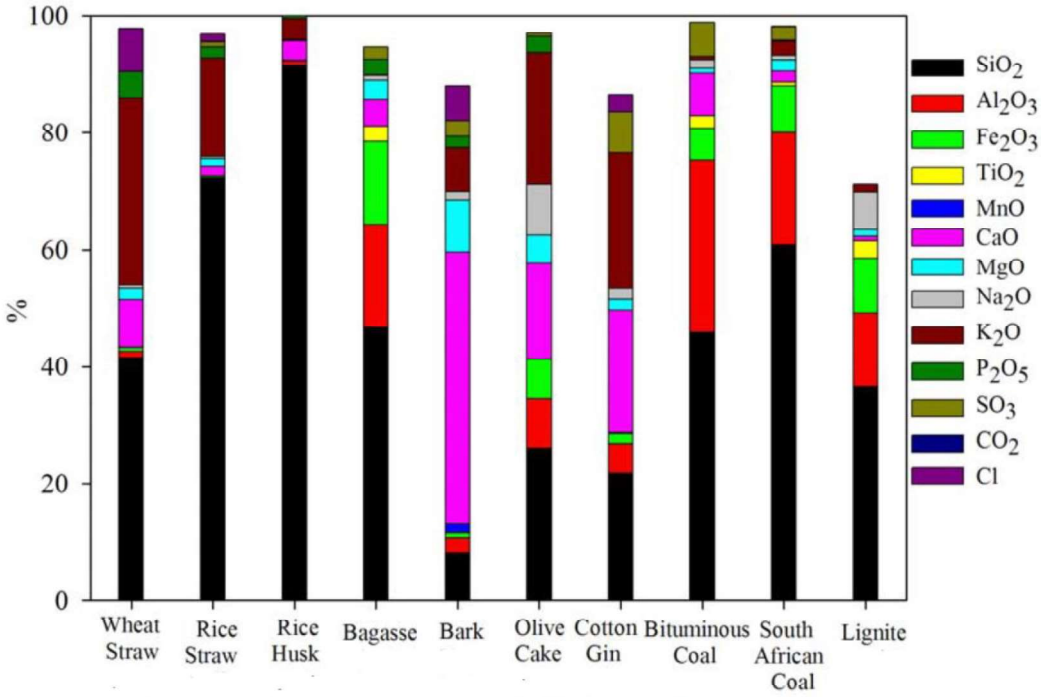

Figure 2.1 Biomass ash compositions [29]

2.1. Operational Problems Associated with Biomass Ash

Figure 2.2 shows schematic of the formation processes of the main ash related problems encountered during biomass combustion.

During biomass combustion, alkali metals undergo complex chemical reactions and transformations and released as alkali metal aerosols ($KCl_{aerosol}$, $K_2SO_{4aerosol}$, $KOH_{aerosol}$, $NaCl_{aerosol}$, $Na_2SO_{4aerosol}$) [31]. When the flue gas temperature decreases, some alkali metal aerosols can condense on furnace walls and form sticky initial slagging layer by diffusion and thermophoresis [32]. Alkali metal aerosols may also condense and deposit on the surface of fly ash forming sticky layer. These sticky ash particles can bond to the initial slagging layer forming alternating layers on the furnace wall. This process is called *alkali induced slagging* [33]. In the case of deposition of these sticky particles on the heat transfer surface, the process is defined as *fouling* [29].

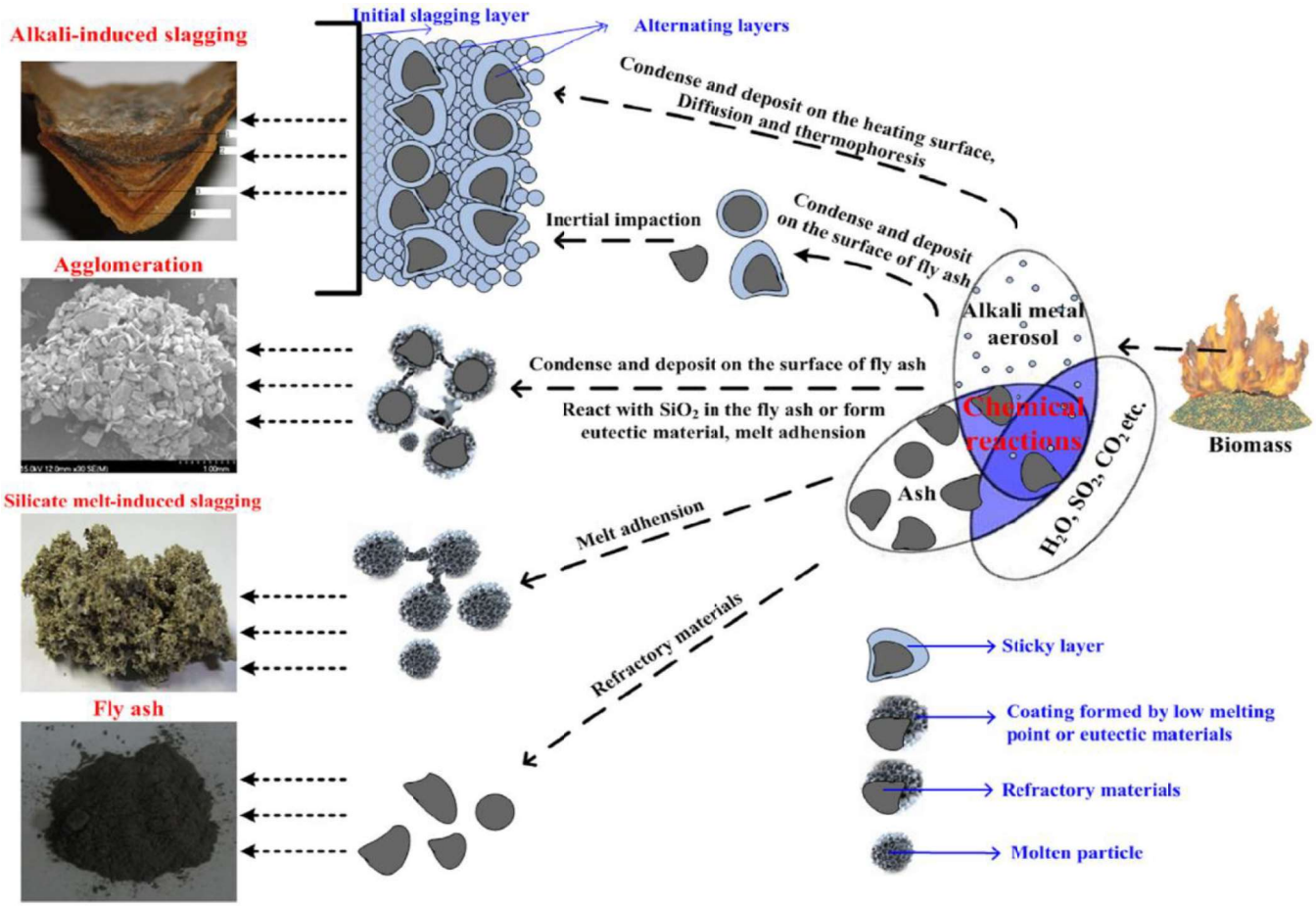

Figure 2.2 Schematic of the formation processes of the main ash-related issues in biomass combustion [33]

Alkali metal aerosols can also react with SiO_2 in the fly ash to form alkali silicates which can melt under typical fluidized bed operation temperatures. These molten ash particles can adhere to each other resulting in *silicate melt induced slagging (ash sintering)* [33,34]. The molten ash particles can also deposit on sand which is used as bed material and result in *agglomeration* [35]. In addition, part of alkali metal aerosols may react with silica component of the bed material forming eutectic minerals, with melting temperatures as low as 650-700˚C, which can also cause agglomeration of particles [36]. Bed agglomeration is a major problem which may result in total de-fluidization of bed material and unscheduled downtime [37]. If sufficient Fe_2O_3 is present in the ash, the rate of formation of agglomerates may be reduced since Fe_2O_3 may react preferentially with the alkali compounds present in the bed [35,38].

Corrosion of heat exchange surfaces is another problem that can be encountered during biomass combustion. Corrosion may occur on heat transfer surfaces when the chlorine content of fuel exceeds 0.1 wt% [29,39,40]. Chlorine containing corrosive deposits damage the heat transfer surfaces at metal temperatures beyond 470˚C which is lower than the typical vapor temperature of steam boilers (~500˚C) [41].

Several indices have been proposed to predict the possible occurrence of ash related problems encountered during biomass combustion [39]. Ash analysis of the fuel is generally used to calculate these indices.

Agglomeration tendency of the fuel can be estimated by calculating *bed agglomeration index (BAI)* using Eqn. (2.1), which is the ratio of iron oxides to sum of potassium and sodium oxides in the fuel ash. Agglomeration is expected to occur when the ratio is less than 0.15 [29].

$$\mathrm{BAI} = \frac{\%\mathrm{Fe_2O_3}}{\%\mathrm{K_2O} + \%\mathrm{Na_2O}} \tag{2.1}$$

Base to acid ratio (B/A), given in Eqn. (2.2), is an indication of the fusion characteristics and slagging potential of ash. If B/A is higher than unity, slagging and fouling is certain to occur during biomass combustion [39]

$$\text{Base to Acid Ratio} = \frac{\%Fe_2O_3 + \%CaO + \%MgO + \%K_2O + \%Na_2O}{\%SiO_2 + \%TiO_2 + \%Al_2O_3} \quad (2.2)$$

Fouling tendency can be also estimated by *alkali index* given in Eqn. (2.3) which expresses the quantity of alkali oxides in the fuel per unit of fuel energy. GCV is expressed in GJ/kg, F_{ash} is the mass fraction of ash in the fuel (dry basis), and F_{K_2O} and F_{Na_2O} are the mass fractions of K_2O and Na_2O in the ash. When alkali index values are in the range 0.17–0.34 kg/GJ fouling is probable, while when these values are greater than 0.34 fouling is virtually certain to occur [42].

$$\text{Alkali Index} = \frac{F_{ash} \times (F_{K_2O} + F_{Na_2O})}{\text{GCV}} \quad (2.3)$$

Alkali index of biomass fuel ash can also be calculated by Eqn. (2.4) which is the ratio of alkali metal oxides to silica in biomass ash. The index higher than unity indicates severe fouling tendency [29].

$$\text{Alkali Index} = \frac{K_2O + Na_2O}{SiO_2} \quad (2.4)$$

The aforementioned ash related issues encountered during biomass combustion could be alleviated by leaching, co-firing of biomass with coal and addition of additives. The first alternative is not economically feasible [18]. Co-firing of biomass with coal has been found to be the most promising alternative; however, it may not be feasible when biomass source and coal mine does not co-exist in the same location [19]. Using additive is an alternative way to prevent operational problems during biomass combustion processes since their usage is eco-friendly, easy to apply and does not require extra maintenance cost for the process [15,20,21].

Additives refer to group of minerals which can change the ash chemistry, convert problematic species to less problematic forms and increase the ash melting temperatures [23]. Depending on reactive components contained in additives, they can be divided into four groups as [43]:

- **Aluminum silica based additives:** Aluminum silica based additives react with potassium compounds and form potassium alumina silicates with high melting temperature. Kaolin, zeolites, emathlite and bentonite are the examples of alumina silicate based additives.
- **Sulfur based additives:** Sulfur based additives convert KCl into K_2SO_4 which is less problematic from the viewpoints of deposition and corrosion.
- **Calcium based additives:** Calcium can dissolve in potassium silicate melts and force potassium release to gas phase. Therefore, more silica will react with calcium with formation of calcium silicates which have higher melting temperatures than potassium silicates. Lime, limestone and marble sludge are common examples of calcium based additives.
- **Phosphorous based additives:** Phosphorous based additives introduce phosphorous in ash which react with potassium forming potassium phosphates. Therefore, available potassium to form potassium silicates with low melting temperatures is reduced. Phosphoric acid is an example of phosphorous based additive.

Additives mixed with fuels and/or added into combustion systems can; (1) increase ash melting temperature by changing ash chemical compositions and transformation chemistry, (2) react with species with low melting temperatures and form less problematic species with higher melting temperatures, (3) capture problematic ash species (i.e., KCl) by physical adsorption [44,45].

Kaolin, which is an alumina based additive, has been identified as promising sorbent for gas phase alkali metal capture at high temperatures. During biomass combustion, the addition of kaolin was shown to increase ash melting temperature of biomass and was verified to be the one of the most effective additive [46-48].

Therefore, in this study, kaolin was selected as additive in the investigation of the elimination of ash related problems encountered in olive residue combustion.

CHAPTER 3

EFFECT OF KAOLIN ADDITION ON ALLEVIATION OF ASH RELATED PROBLEMS

High potassium content of the olive residue, which is the fuel under investigation in this study, is known to be responsible from ash related problems encountered during its combustion [5]. In order to investigate the possibility of elimination of these problems by kaolin addition, pathway of potassium during biomass combustion and its reaction with kaolin should be investigated in detail.

3.1. Pathway of Potassium during Biomass Combustion and its Capture by Kaolin Addition

During biomass combustion, potassium species are released and transported either in the form of solid particles or vapor species in the combustion gas [33]. Part of potassium reacts with fuel ash forming potassium silicates and potassium alumina silicates [31]. The remaining potassium is released in gas phase mainly as KCl(g) and KOH(g) depending on the biomass composition [49].

The chlorine content of the biomass dictates the amount and type of potassium containing species released during combustion [29, 31,49-51].

- If K/Cl molar ratio is lower than unity, high chlorine content promotes the release of KCl(g) while no KOH(g) is formed and excess chlorine is released in the form of HCl(g) [33, 50].

- If K/Cl ratio is unity, KCl(g) is the dominant product. However, the relative proportion of KOH(g) rises when the amounts of K and Cl are lowered which is attributed to the reverse chlorination reaction given below [31,33,50];

$$KOH(g) + HCl(g) \longleftrightarrow KCl(g) + H_2O(g) \qquad R1$$

- If K/Cl ratio is higher than unity, at temperatures above 800˚C, the excess potassium goes through hydration reaction forming KOH(g) in moist environment [47,50] while below this temperature $K_2CO_3(g)$ is formed by carbonation reaction given below [31,33];

$$2\ KOH(g) + CO_2(g) \longleftrightarrow K_2CO_3(g) + H_2O(g) \qquad R2$$

$K_2CO_3(g)$ can also react with HCl(g) to form KCl(g) with the following reaction;

$$K_2CO_3(g) + 2HCl(g) \longleftrightarrow 2KCl(g) + CO_2(g) + H_2O(g) \qquad R3$$

During combustion, $SO_2(g)$ or $SO_3(g)$ is formed by oxidation of sulfur available in the biomass fuel. Potassium species released as KCl(g), KOH(g) and $K_2CO_3(g)$ can react with SO_2 or SO_3 gases to form potassium sulfate via sulfation reactions [33, 52]:

$$2\ KCl(g) + SO_2(g) + ½\ O_2(g) + H_2O(g) \longrightarrow K_2SO_4(g) + 2\ HCl(g) \qquad R4$$

$$2\ KOH(g) + SO_2(g) + ½\ O_2(g) \longrightarrow K_2SO_4(g) + H_2O(g) \qquad R5$$

$$K_2CO_3(g) + SO_2(g) + ½\ O_2(g) \longrightarrow K_2SO_4(g) + CO_2(g) \qquad R6$$

where the corresponding equations for SO_3 can be obtained by replacing SO_2 + ½ O_2 with SO_3. Sulfation rate of KCl was found to be limited by the availability of SO_3 at 900-1100˚C. Therefore, the oxidation of SO_2 to SO_3 is the rate limiting step in sulfation reactions [53, 54]. Both KCl(g) and $K_2SO_4(g)$, with condensation temperatures of 770 and 745˚C [53], respectively, may form deposits on heat transfer surfaces. However, K_2SO_4 is less corrosive compared to KCl [41] which makes sulfation of KCl important for elimination of corrosion problems. The rate of corrosion is significantly affected by the availability of sulfur for sulfation reactions. Although S/Cl ratio of 0.5 is theoretically enough for sulphation of all KCl according to R4, higher S/Cl ratio is needed due to consumption of available SO_3 or SO_2 by calcium compounds ($CaCO_3$,

CaO) and KOH [29, 54]. Salmenoja and Makela [55] stated that to avoid or minimize superheater corrosion in biomass fired boilers, the S/Cl ratio should at least be 2.0 preferably over 4.0.

To eliminate ash related problems caused by presence of KCl(g), KOH(g) and K_2SO_4(g), kaolin can be added to capture and convert these species into less problematic species. Kaolin refers to a group of clay minerals whose most common mineral is kaolinite ($Al_2Si_2O_5(OH)_4$). When kaolin is heated to 450–600˚C, water is released and kaolinite is transported to an amorphous mixture of alumina and silica called meta-kaolinite as [15];

$$Al_2Si_2O_5(OH)_4 \longrightarrow Al_2O_3.2SiO_2(g) + H_2O(g) \qquad \text{R7}$$

The meta-kaolinite can adsorb and react with KCl, KOH and K_2SO_4 to form of crystalline products $KAlSiO_4$ (kalsilite) and $KAlSi_2O_6$ (leucite) which have melting temperatures of 1600 and 1500°C, respectively, via reactions R8-R13 [14-16, 60]. The overall reactions between potassium species and meta-kaolinite can be presented as [46,47,56];

$$Al_2O_3.2SiO_2(s) + 2\ KCl(g) + H_2O(g) \longrightarrow 2\ KAlSiO_4(s) + 2\ HCl(g) \qquad \text{R8}$$

$$Al_2O_3.2SiO_2(s) + 2\ KCl(g) + 2\ SiO_2(s) + H_2O(g) \longrightarrow 2\ KAlSi_2O_6(s) + 2\ HCl(g) \qquad \text{R9}$$

$$Al_2O_3.2SiO_2(s) + 2\ KOH(g) \longrightarrow 2\ KAlSiO_4(s) + H_2O(g) \qquad \text{R10}$$

$$Al_2O_3.2SiO_2(s) + 2\ KOH(g) + 2\ SiO_2(s) \longrightarrow 2KAlSi_2O_6(s) + H_2O(g) \qquad \text{R11}$$

$$K_2SO_4(s) + Al_2O_3.2SiO_2(s) \longrightarrow 2\ KAlSiO_4(s) + SO_3(g) \qquad \text{R12}$$

$$Al_2O_3.2SiO_2(s) + K_2SO_4(s) + 2\ SiO_2(s) \longrightarrow 2\ KAlSi_2O_6(s) + SO_3(g) \qquad \text{R13}$$

As can be seen in these reactions, kaolin reduces the concentrations of troublesome alkalis in the flue gas and ashes and also forms refractory potassium alumina silicates. Therefore, ash sintering, slagging agglomeration and corrosion problems can be eliminated with kaolin addition.

3.2. Literature Review on Combustion Studies of Biomass with Kaolin Addition

The effect of kaolin addition on ash sintering, slagging, corrosion tendency of biomass fuels and emission of acidic gaseous species were investigated in different combustion systems in the literature. Majority of these studies were conducted in laboratory oven where fuel or fuel ash was mixed with kaolin at different weight percentages and the mixture was heated to a certain temperature to see the effect of kaolin addition and the temperature on the ashes formed at the end of operation.

Wang and co-workers conducted several studies [16,22,44,45,57] with different biomasses on the effect of kaolin addition on sintering. In the experiments, barley straw and wheat straw ash obtained at 550˚C was mixed with kaolin (4% by wt.) while rye straw and husk fuels were mixed with kaolin and ashed at 550˚C in laboratory oven. The ashes were further sintered at 700, 800, 900 and 1000˚C. The sintered residues were analyzed by SEM-EDX and XRD. In SEM images of ash-kaolin mixtures, no clear melting was observed which was considered to be due to increase in alumina content of ash with kaolin addition. Moreover, leucite ($KAlSi_2O_6$) and kalsilite ($KAlSiO_4$) crystals with high melting temperatures were detected in XRD analysis. Furthermore, sintering degree of ashes were graded by visual observation and ash fusion temperatures were determined. Decrease in sintering degree was observed with kaolin addition which was also confirmed by increase in ash fusion temperatures of ashes via addition of kaolin. Several researchers also reported the increase in ash fusion temperatures of biomass fuels with kaolin addition [25,58,59].

In the study of Schmitt and Kaltschmitt [60], wheat straw and willow wood fuels with 1 and 2% kaolin were pelletized and ashed at 550˚C. 0.5 gram of ashes were then heated up to 1000˚C in laboratory furnace to investigate the effect of kaolin addition on sintering degree. The sintering degree of straw ash was found to decrease by 1% kaolin addition while no further improvement was observed with 2% kaolin addition. In XRD analyses of ashes of wheat straw with kaolin addition, kalsilite and leucite crystals with high melting temperatures were detected confirming anti-sintering effect of kaolin addition. Konsomboon et al. [56] investigated the optimum kaolin ratio

required to capture all available potassium released during combustion of empty fruit bunch (EFB). About 6 g of sample (EFB and EFB-kaolin mixture) was loaded into sample holder of a laboratory furnace which was preheated to 700, 800 and 900˚C. The amounts of kaolin used were 8% and 16% by weight based on dry weight of EFB, which were equivalent to one and two times of the theoretical kaolin requirement to capture all potassium originally present in the EFB. The researchers pointed out that the furnace temperature considerably affected the amount of the evaporated potassium species during combustion of EFB. With the increase in operating temperature, lower potassium retention in EFB ash was monitored. It was observed that at 700 and 800°C, 8% kaolin addition was sufficient to completely retain potassium in the solid phase. However, twice the amount was needed for 900°C due to the large amount of volatilisable potassium.

Sommersacher et al. [61] studied the effect of kaolin addition on ash melting and corrosion problems encountered during combustion of spruce and straw. In their study, they first conducted wet chemical analyses on pure biomasses. On the basis of this analysis, theoretical mixing calculations of promising kaolin ratios were performed. These theoretical mixtures were evaluated with fuel indices and thermodynamic equilibrium calculations (TEC). Fuel indices provided the first information regarding high temperature corrosion (2S/Cl) and ash melting tendency (Si + P + K)/(Ca + Mg + Al). TEC was used for a qualitative prediction of the release of volatile and semivolatile elements (K, Na, S, Cl, Zn, Pb) and the ash melting behaviour. In addition, experiments were also performed in a lab-scale reactor for validation of theoretical calculations. The validation of the ash melting behavior was conducted by conducting standard ash melting test. For spruce 0, 0.2, 1, and 3 wt % kaolin, whereas for straw 0, 1, 4, and 7 wt % kaolin addition were selected for investigation. For spruce 0.2 wt % kaolin and for straw 4 wt % kaolin were evaluated to be the optimum kaolin addition ratios to considerably reduce aerosol emissions and substantially improve the ash melting behaviour.

Steenari and co-workers [15,62] investigated the effect of kaolin on ash sintering behaviour of straw, wheat, barley, oat grains, rapeseed, rapeseed press residue,

bluegrass seeds, bluegrass waste, red fescue waste and ryegrass waste. Fuel ashes obtained at 550˚C were mixed with kaolin (4% w/w dry biomass) and further heated in laboratory oven at 700˚C, 800˚C, 900˚C, 1000 ˚C. The slag formation was then estimated visually according to a graded scale: (1) not or very little affected; (2) affected by partial sintering but still retaining a porous, brittle structure; (3) sintered; (4) very hard, sintered structure; (5) melted. The amount of additive used in the tests was chosen to be three times the stoichiometric amount needed for the expected reactions as: 4-5.5% for wheat sorting residue, barley sorting residue, and oats grains; 7-10% for rapeseed, red fescue residues, and rye grass residues; and 15-30% for the remaining fuels. Kaolin was found to serve as a good additive to prevent the formation of slag. The researchers stated that the results obtained solely in a laboratory oven should not be regarded completely as non-representative of a real combustion situation as several of these fuels were mixed with additives and were pelletized and fired in the Bioagro boilers with good results, and the simple tests used in their study worked fine for evaluating pellet recipes.

In some of the studies, in addition to ash analyses, the change of composition of the flue gas with kaolin addition was also investigated. Some researchers focused on the change of the pathway of chlorine released during biomass combustion with kaolin addition [14, 63-65]. In these studies, decrease in chlorine in ash and increase in HCl in flue gas were observed with kaolin addition which was due to the ability of kaolin to restrain more potassium in the ash, leading chlorine to be released in the form of HCl(g).

The effect of kaolin addition on deposit formation during combustion of wood pellets was studied by Paneru and co-workers [66] in a drop tube furnace. The pulverized fuel was mixed with 1.5 and 2% kaolin prior to combustion experiments. The deposit samples were collected using deposit probes located at 1.5 m down the burner in the temperature range ≥1200°C which is the temperature range relevant to pulverized firing systems. Feeding kaolin together with biomass was found to facilitate the capture of gaseous potassium species as soon as they are released forming stable alkali alumina silicate with high melting temperature which would otherwise form alkali

silicates with low melting temperature.

Another study on the effect of kaolin addition on deposit formation was carried out by Madhiyanon et al. [67] in a 150 kW_{th} pilot scale grate-fired combustor. Deposits were collected by deposit probes during combustion of oil-palm empty fruit bunch (EFB). With the addition of 8% kaolin, it was monitored that the probe surface temperature remained unchanged, and the hindrance of heat transfer was resolved indicating the efficient ability of kaolin to counteract the deposit formation. SEM-EDX mapping together with XRF analyses performed on deposits revealed an accomplishment in the formation of high-melting-point eutectics (potassium alumina silicates), resulting in significantly diminished deposition and sintering tendencies with the addition of kaolin.

Agglomeration is an important problem especially in fluidized bed systems as it may result in total de-fluidization of bed material and un-scheduled shut-down of the system. Öhman *et al*. [68] investigated the role of kaolin in prevention of bed agglomeration during fluidized bed combustion of pelletized wheat straw and bark. The experiments were performed in a 5 kW bench scale fluidized bed reactor with a normal sand bed and with a bed containing sand and 10% (w/w) kaolin powder (< 200 μm). During experiments, representative samples of the bed material were collected. These samples, as well as the final agglomerated particles, were characterized with XRD and SEM/EDS analysers. Based on the semi-quantitative EDS analyses of ash and bed particles, the melting behaviour of the particles was estimated by extracting corresponding data from K_2O-SiO_2-Al_2O_3 phase diagram. The compositions of the coatings were altered toward higher melting temperatures with kaolin addition, mainly because of their decreased potassium and increased alumina content. Moreover, initial bed agglomeration tendencies were determined by controlled fluidized bed agglomeration test. By adding small amounts of kaolin to the bed when firing wheat straw, the critical temperature for initial bed agglomeration was increased by over 100°C. The corresponding increase with bark as fuel was only about 10°C. Both these observations were in agreement with the melting behaviour extracted from the relevant phase diagrams.

Limited number of studies was conducted in pilot scale fluidized bed systems. Addition of kaolin on agglomeration and deposit tendency of wood chips was studied by Davidsson *et al.* [69] in a 35 MW circulating fluidized bed heat and power plant. In the experiments, natural sand was used as bed material and kaolin was supplied through the lime supply system to the particle seal in the form of a fine powder. The samples of bottom and fly ash were collected and analysed for elemental composition, water solubility and mineralogical composition. As majority of the kaolin was observed to be carried by the flue gases to the electrostatic filter rather than staying in the bed, potassium content was found to decrease in the bed and bottom ash while it was found to increase in the fly ash. Even though a small fraction of the kaolin stayed in the furnace, the results revealed that kaolin addition decreased the tendency of agglomeration and deposit formation.

In a comprehensive study conducted by Davidsson and co-workers [70] in *Chalmers University of Technology*, wood chips and wood pellets were fired together with straw pellet in a 12 MW_{th} circulating fluidized bed combustor (CFB) and the effects of addition of elemental sulphur, ammonium sulphate and kaolin to a bed of silica sand, as well as use of olivine sand and blast-furnace slag as alternative bed materials on the biomass combustion characteristics were investigated. The agglomeration temperature, composition and structure of bed-ash samples were examined. The flue-gas composition, including gaseous alkali chlorides, was measured in the hot flue gases and in the stack. Particles in the flue gas were collected and analysed for size distribution and composition. Deposits were collected on a probe in hot flue gases and their amount and composition were analysed. Addition of kaolin was found to reduce KCl concentration in the flue-gas to an acceptable level, which led to little or no deposition of KCl on superheater tubes. It was concluded that among the mitigation methods tested, addition of kaolin was the best one to counteract the agglomeration problem.

In the open literature, to the author's knowledge, only two studies exist on the effect of kaolin addition on slagging/fouling and agglomeration tendency of olive residue, which is the fuel under investigation in this study. Llorente and his colleagues [24]

studied the effect of additives (kaolin, limestone, lime, dolomite, calcined dolomite, ophite and alumina and silicon) on sintering tendency of five different biomasses (thistle, brassica, barley straw, almond shell and *orujillo (de-oiled and dried olive residue*)). Sintering tests of the mixtures were carried in a laboratory oven. The additives were mixed with biomass ash obtained at 550˚C at different mixing ratios: 0.125, 0.25, 0.5, 1 and 2 g of additive per g biomass ash. The mixtures were then heated to 1000˚C in the oven. The mixture with 1 g kaolin/1 g biomass ash was determined as optimum ratio to reduce sintering tendency of orujillo from weak sinter to loose ash. In XRD pattern of the ash, $KAlSiO_4$, SiO_2, $Ca_2MgSi_2O_7$ minerals which have high melting temperatures were detected confirming good potential of kaolin to reduce ash sintering tendency.

Vamvuka et al. [71] investigated effect of kaolin addition on slagging/fouling and agglomeration tendency of olive kernel and olive tree wood. Combustion experiments were carried out in a lab-scale fluidized bed combustor. Na-feldspar (NaAlSi3O8) was used as bed material. The bed temperature was kept at 800˚C during each experiment. Fuels and fuels mixed with 5% kaolin additive were combusted in the FBC system and bed and fly ash particles were analyzed by SEM-EDX and AAS and XRD, respectively. Bed ash particles contained mainly alumina and silica followed by significant amounts of Ca, Mg and K. No agglomeration was observed in SEM images. With kaolin addition, concentration of alkalis in fly ash was found to decrease due to the retention of alkalis in bed particles or their possible release with flue gas.

In neither of these above-mentioned studies conducted with olive residue, flue gases during combustion was detected. However, to have a complete picture on the pathway of potassium during combustion, both ashes and the flue gases should be examined. This study aims to fill this gap in the literature. In an attempt to achieve this objective, TGA-FTIR combustion analyses and quantitative and qualitative analyses of ashes of olive residue and olive residue-kaolin mixtures were carried out by XRF, XRD and SEM-EDX analyses.

CHAPTER 4

EXPERIMENTAL

4.1. General

In the first part of this chapter, materials used in experiments and their characteristics including proximate, ultimate and ash analyses are reported. This is followed by detailed description of the experimental methods used in this study.

4.2. Materials

Experiments were carried out with olive residue and olive residue-kaolin mixtures. Representative samples of olive residue (Figure 4.1) were subjected to proximate, ultimate and ash analyses. Proximate analysis of olive residue was performed by LECO TGA-701. Ultimate analysis was carried out with LECO CHNS-932. Calorific value was measured by using AC-500 bomb calorimeter. Ash content was determined by XRF analyzer. Weak acid soluble potassium in as received olive residue was determined according to TS 1651 ISO 1952 Standard. Proximate, ultimate and ash analyses of olive residue together with its calorific value are briefly summarized in Table 4.1.

Figure 4.1 Photograph of olive residue and kaolin additive

Table 4.1 Characteristics and ash analysis of olive residue

Proximate Analysis (%, as received basis)	
Moisture	6.87
Ash	5.65
Volatile Matter	69.70
Fixed Carbon	17.81
Ultimate Analysis (%, as received basis)	
Carbon	47.8
Hydrogen	6.13
Nitrogen	2.02
Oxygen	31.3
Combustible sulfur	0.25
Total sulfur	0.25
Chlorine	0.15
Ash	5.65
Moisture	6.87
Weak acid soluble K in OR (%, as received basis)	0.71
Calorific Value (As received basis)	
LHV, MJ/kg	18.1
Ash Analysis (%)	
SiO_2	9.30
Al_2O_3	3.60
Fe_2O_3	4.47
CaO	27.16
MgO	4.59
Na_2O	1.58
K_2O	39.57
TiO_2	0.33
P_2O_5	6.40
MnO	0.08

In this study, Kaolin 190 was used as additive. Chemical composition of kaolin is tabulated in Table 4.2.

Table 4.2 Chemical composition of Kaolin 190 (%)

SiO_2	46.74
Al_2O_3	37.45
Fe_2O_3	0.47
CaO	0.36
MgO	0.01
Na_2O	0.01
K_2O	0.84
TiO_2	0.80
SO_4	0.22
LOI	13.14

4.3. Experimental Method

4.3.1. TGA-FTIR Analyses

In the present work, thermogravimetry (TGA) / differential thermogravimetry (DTG) were used to determine the effect of kaolin on combustion characteristic of olive residue. It is a rapid, inexpensive and simple method that has been widely used in investigation of combustion behaviour of various fuels and evaluation of the relative burning properties of fuel samples [72-75]. In order to determine evolved gases during combustion experiments, TGA system was coupled with Fourier transform infrared (FTIR) spectrometer, which has many applications in the open literature [76-82]. Schematic diagram of TGA-FTIR system is shown in Figure 4.2. Experimental setup consists of Perkin Elmer Pyris STA 600 Thermogravimetric Analysis and Spectrum 1 FT-IR Spectrometer. FTIR spectra was collected with 4 cm^{-1} resolutions, in the range of 4000-700 cm^{-1} IR absorption band.

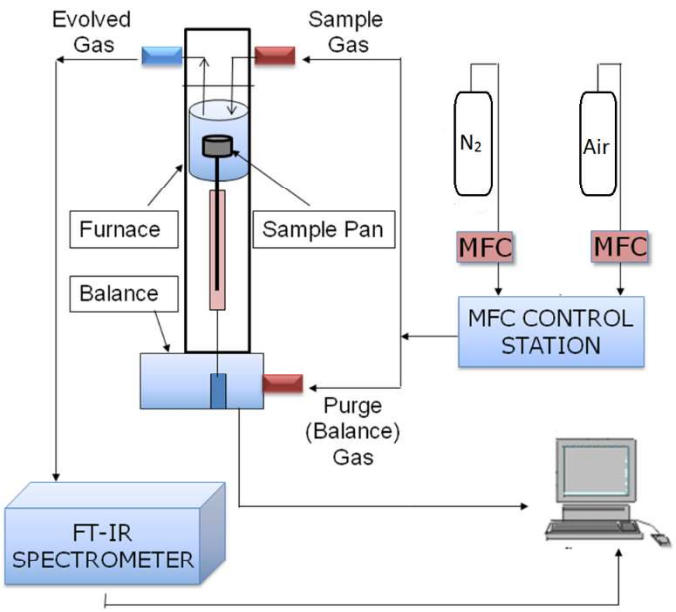

Figure 4.2 Schematic diagram of TGA-FTIR system [83]

After both olive residue and kaolin were sieved to obtain particle size less than 100µm, about 15 mg of olive residue and olive residue-kaolin mixtures with additive to mixture ratio of 2%, 4% and 8% on as received basis were held initially at room temperature for 1 minute and then heated with a heating rate of 40˚C/min from 25˚C to 950˚C during each experiment. In the experiments, 50 ml/min N_2 gas was sent to purge as balance gas and 60 ml/min air was sent to sample.

TGA and DTG profiles obtained during combustion experiments were used to determine some characteristic parameters namely initial decomposition temperature (T_{in}), peak temperature (T_{max}), ignition temperature (T_{ig}) and burnout temperature (T_b). T_{in} represents the initiation of weight loss and is defined as the temperature at which the rate of weight loss reaches 1 %/min after initial moisture loss peak in DTG profile [84]. T_{max} is the point at which maximum reaction rate occurs. Ignition temperature T_{ig} is defined as the temperature at which fuel starts burning [74,76,85]. The last characteristic temperature considered is burnout temperature, which represents the temperature where sample oxidation is completed. It is taken as the point immediately before reaction ceases when the rate of weight loss is 1 %/min [72]. Theoretical DTG

curves of the olive residue with and without kaolin addition samples were plotted in order to investigate influence of kaolin ratio on characteristic temperatures of olive residue.

A linear relation between spectral absorbance at a given wavenumber and concentration of gaseous components is given by Beer's Law. In this study, the points of absorbance at a certain wavenumber are plotted against temperature in order to obtain a formation profile for each evolved gas observed in the spectra during experiments. The IR wavenumbers of CO_2, CO, HCl, SO_2, COS and CH_4 are 2360, 2112, 2936, 1340, 2042 and 3016 cm^{-1}, respectively [83]. Formation profiles of NO_x related species such as NO and NO_2 are not reported due to overlap of their absorption bands with the characteristic absorption bands of water in the range of 3900-3500 and 1900-1350 cm^{-1}.

4.3.2. Sintering Tests

Sintering tests of olive residue and olive residue-kaolin mixtures were performed in order to visually observe the effect of kaolin on ash sintering characteristics of olive residue. Olive residue with and without kaolin addition are burned at 900˚C in a preheated laboratory furnace. The ash residues remaining in the crucibles were assessed in terms of sintering behaviors. The sintering degree of the residues was then graded with the following scale: (1) loose ash without aggregates and slag formation, (2) slightly sintered ash with an easily broken fragile structure, (3) hard sintered ash with partial melting, (4) very hard sintered ash related to formation of heavy sinters and slag and (5) completely melted [45].

4.3.3. XRF and XRD Analyses

The quantitative and qualitative ash analyses of olive residue and olive residue-kaolin mixtures obtained at 900˚C were carried out by XRF [Rigaku ZSX Primus II] and XRD [Rigaku Ultima-IV] analyzers. XRF analyses were carried out on dried (at 105-

110˚C) and pelletized samples. In XRD analysis, powder sample was distributed uniformly on the sample holder to ensure a flat upper surface. The analyses were performed with scan rate of 5 to 70˚ and scan speed of 1˚/min.

4.3.4. SEM-EDX Analyses

The morphology and microchemistry of the ashes of olive residue and olive residue-kaolin mixtures obtained at 900˚C in preheated furnace were examined by SEM-EDX. The ash samples were embedded into epoxy, which was cross-sectioned and polished. The samples and their cross sections were coated with carbon and carefully examined by SEM–EDX. For selected samples and scan areas, EDX semi quantitative spot/area analyses were performed. The SEM images and results of EDX analyses are presented in Appendix A.

CHAPTER 5

RESULTS AND DISCUSSIONS

5.1. General

This thesis study is based on investigation of the effect of kaolin addition on combustion characteristic of olive residue. Effect of kaolin addition on combustion characteristic of olive residue is studied by TGA-FTIR analyses. Results of TGA-FTIR analyses of olive residue and olive residue-kaolin mixtures are analyzed by using weight loss and derivative weight loss (TGA/DTG) profiles. Formation profiles of the evolved gases identified in FTIR spectra of the fuel samples are also presented. Effect of kaolin addition on ash sintering behavior of olive residue is analyzed by results of sintering and ash fusion temperature determination tests and also through XRD, XRF and SEM-EDX analyses performed on ash samples. The experiments were carried out by burning olive residue with 2%, 4% and 8% by wt. kaolin. In light of the results of these analyses, optimum kaolin addition ratio was determined.

5.2. TGA-FTIR Analyses of Combustion of Olive Residue and Olive Residue-Kaolin Mixtures

TGA and DTG profiles of combustion of olive residue and olive residue with kaolin addition are illustrated in Figure 5.1. Three main weight loss steps appear in all weight loss profiles irrespective of kaolin addition ratio. The first weight loss step within 25-150°C temperature range is attributed to moisture release. The main weight loss occurs in the second stage within the temperature range of 170-400°C where mainly devolatilization of hemicellulose and cellulose component and their subsequent

ignition takes place [81]. This is followed by the third stage weight loss which is associated with char combustion within the temperature range of 400-640°C. In this range, weight loss rate decreases with increasing kaolin addition which is considered to be due to suppression of combustion by kaolin.

TGA and DTG profiles obtained during combustion experiments were used to determine characteristic parameters such as initial decomposition temperature (T_{in}), peak temperatures ($T_{max,1}$, $T_{max,2}$), ignition temperature (T_{ig}) and burnout temperature (T_b). These parameters are tabulated in Table 5.1. As can be seen from the table, combustion parameters are not significantly affected by kaolin addition. However, rate of weight loss during char combustion decreases with increasing kaolin addition as also illustrated in DTG curves.

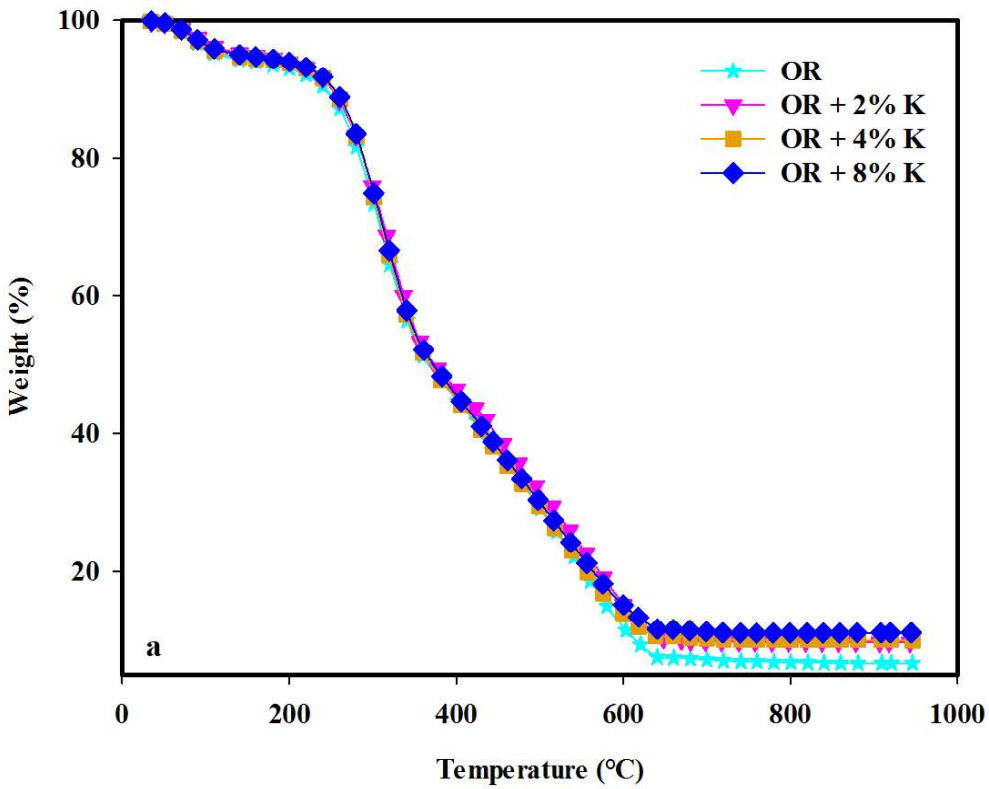

Figure 5.1 TGA (a) and DTG (b) profiles of combustion of olive residue (OR) and olive residue-kaolin (K) mixtures (cont'd)

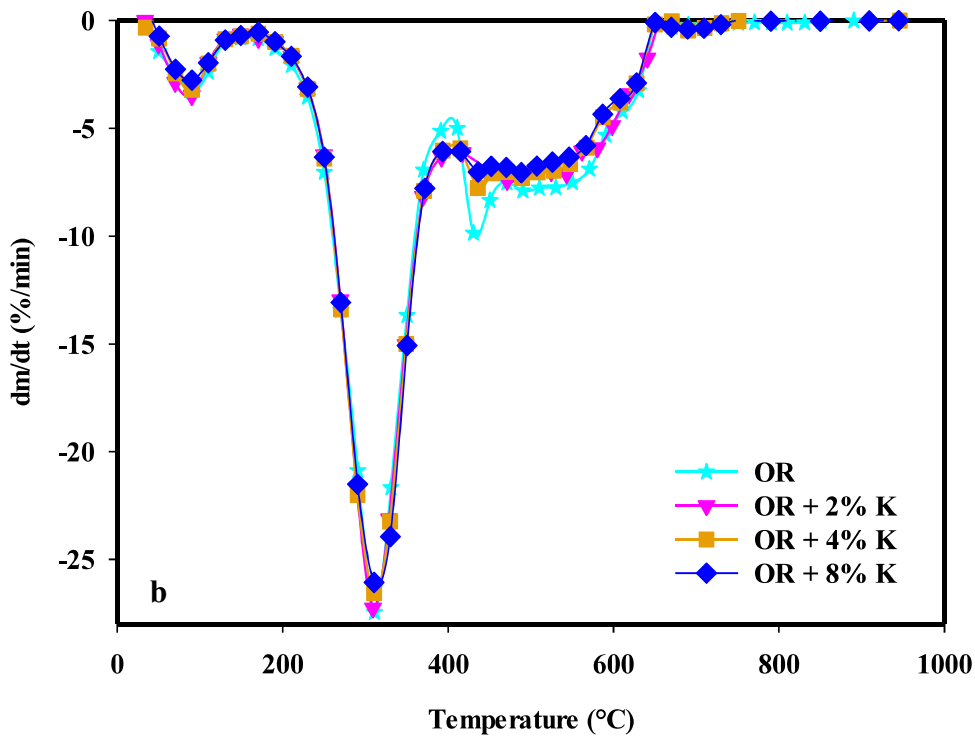

Figure 5.1 TGA (a) and DTG (b) profiles of combustion of olive residue (OR) and olive residue-kaolin (K) mixtures

Table 5.1 Combustion characteristics of olive residue (OR) and olive residue-kaolin mixtures

	OR	**OR+2% Kaolin**	**OR+4% Kaolin**	**OR+8% Kaolin**
T_{in} (˚C)	185.8	189.3	193.4	190.7
T_{max-1} (˚C)	315.6	311.7	313.9	316.8
T_{max-2} (˚C)	432.4	436.3	429.0	429.6
T_b (˚C)	638.3	640.1	631.1	639.1
$(dm/dt)_{max-1}$ (%/min)	28.1	27.0	26.7	26.3
$(dm/dt)_{max-2}$ (%/min)	10.7	8.2	8.0	7.2
T_{ig} (˚C)	256.0	269.2	282.4	277.3
Total weight loss up to 950˚C	93.2	92.8	90.0	88.9

The points of absorbance at a certain wavenumber are plotted against temperature in order to obtain a formation profile for each evolved gas observed in the spectra during experiments. Figure 5.2 displays evolution of gaseous species including CO_2, CO,

SO_2, HCl, COS and CH_4 during combustion of olive residue and olive residue-kaolin mixtures. As illustrated in this figure, the major contributor to the evolved gas is found to be CO_2 with its higher absorbance intensity.

Both CO_2 and CO evolution is observed to initiate at around 300°C and continues up to the end of combustion. Although kaolin addition does not significantly affect formation profile of CO_2, increase in kaolin ratio results in higher absorbance of CO. This is considered to be due to decrease in burning quality as O_2 diffusion decreases through the mixture layer with higher kaolin ratio.

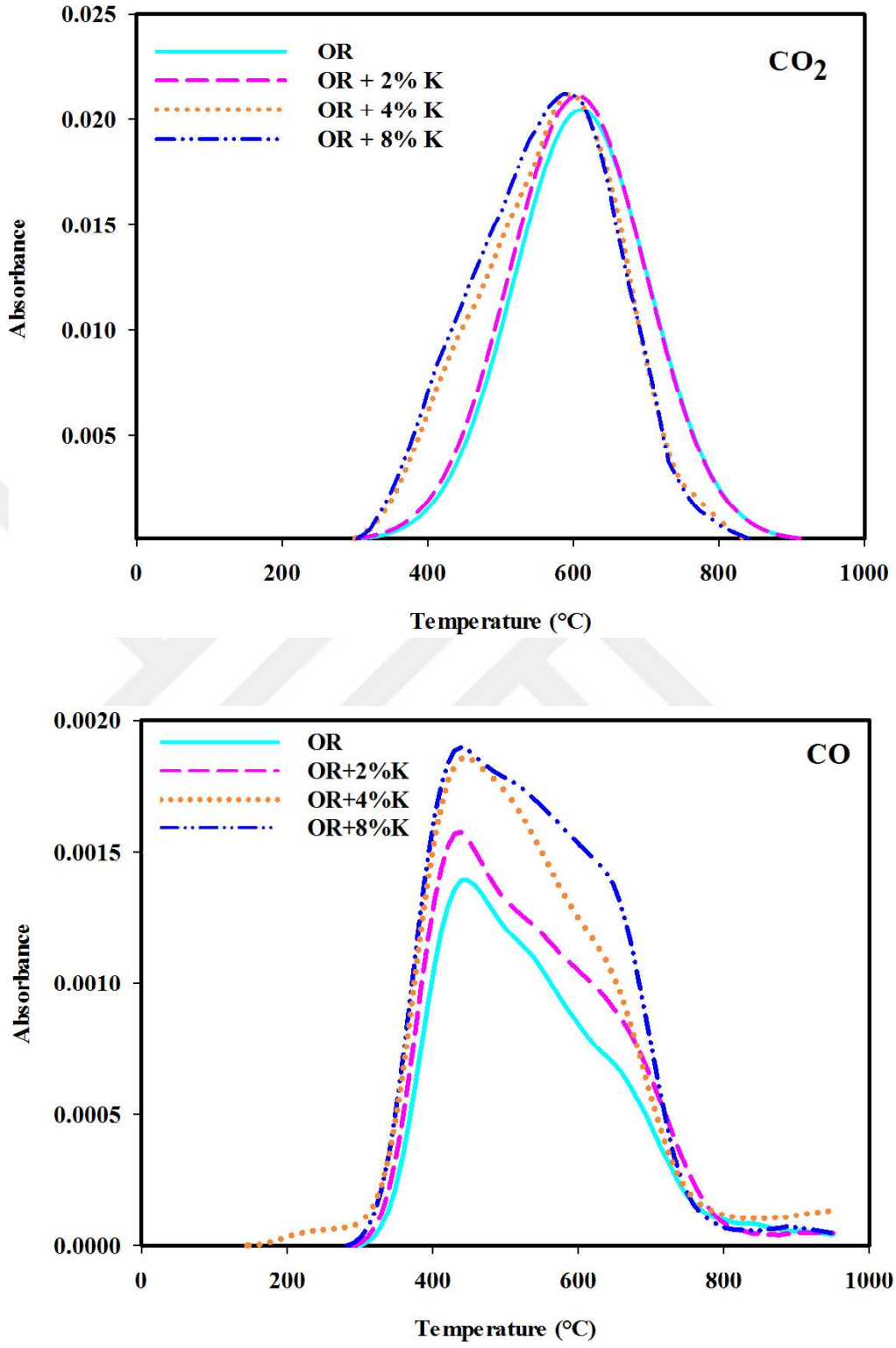

Figure 5.2 Evolved gas formation profiles of olive residue (OR) and olive residue-kaolin (K) mixtures during combustion tests (cont'd)

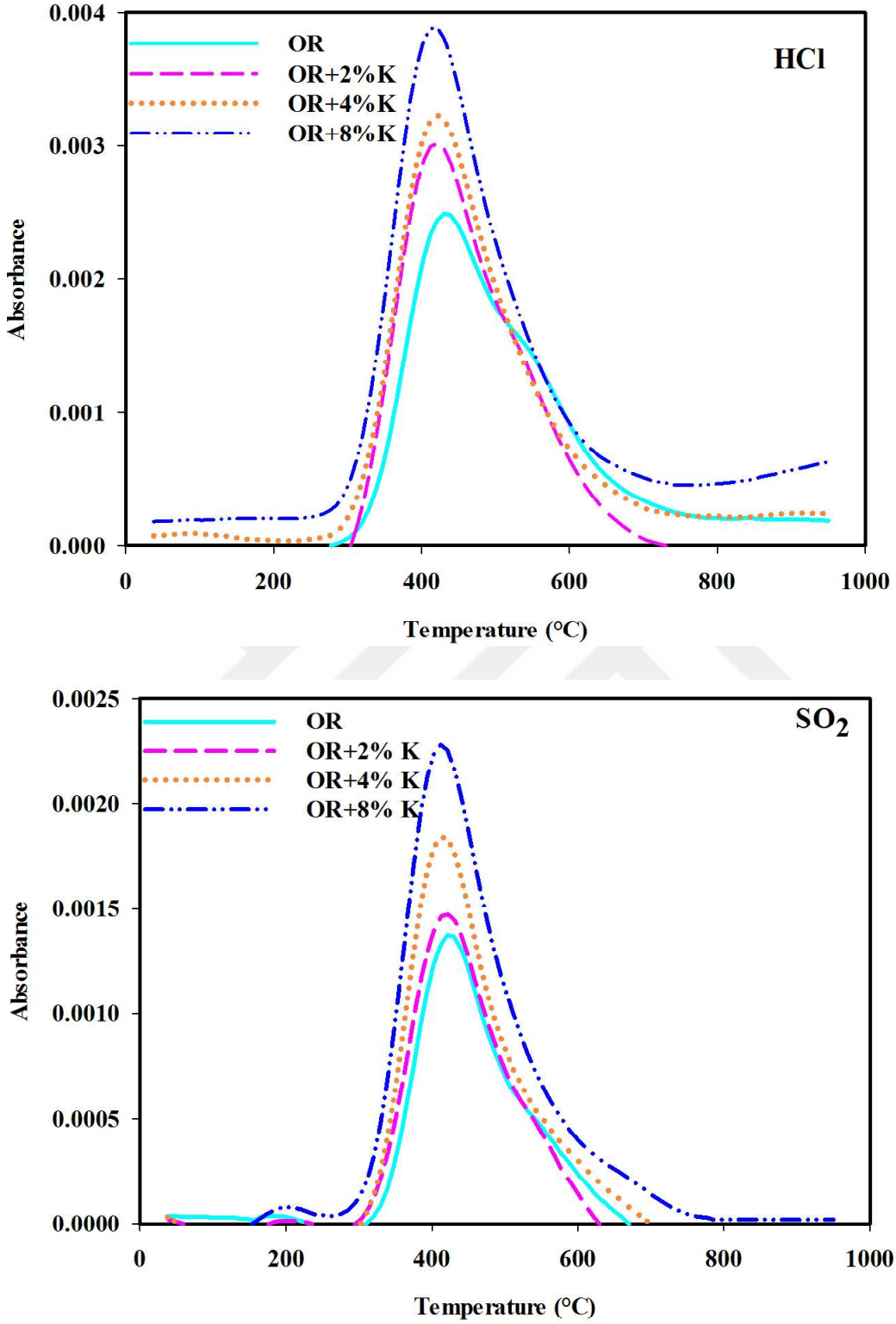

Figure 5.2 Evolved gas formation profiles of olive residue (OR) and olive residue-kaolin (K) mixtures during combustion tests (cont'd)

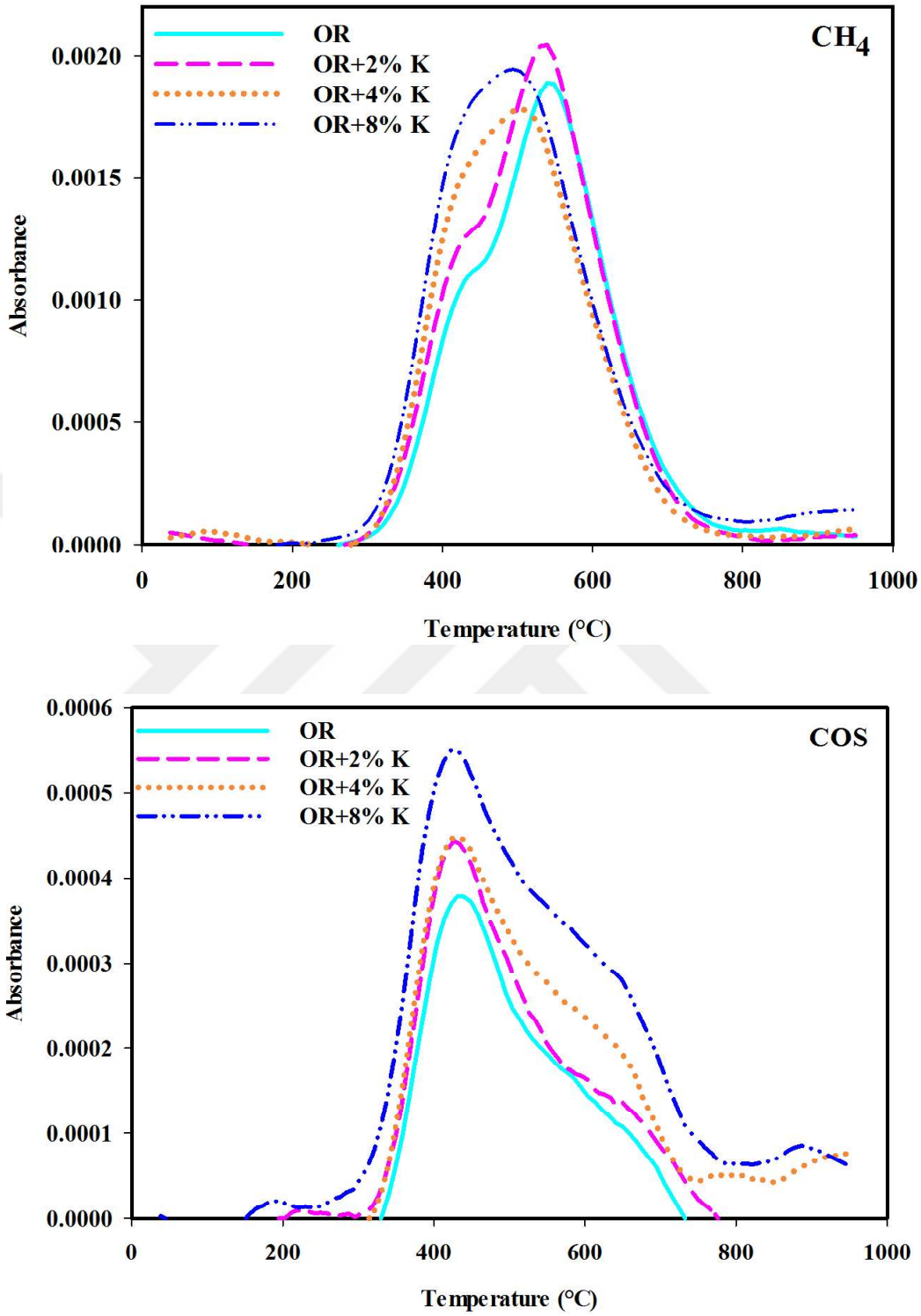

Figure 5.2 Evolved gas formation profiles of olive residue (OR) and olive residue-kaolin (K) mixtures during combustion tests

Formation profiles of HCl(g) and SO_2(g) are also influenced by kaolin addition. The effect can be demonstrated by considering reaction paths of potassium without and

with kaolin addition shown in Figure 5.3. As can be seen from figure, without kaolin addition, potassium in the fuel goes through chlorination and hydration reactions. Chlorination is expected to be the main pathway of release of Cl with molar K/Cl ratio (4.29) higher than unity during combustion of olive residue at 900°C [33,21]. However, due to low Cl and S and high moisture content of olive residue, hydration reaction becomes dominant leading to KOH(g) formation [51]. Sulfation of KOH(g) and KCl(g) is limited by both low Cl and S contents and low oxidation rate of SO_2(g) to SO_3(g). Part of the KOH(g) remaining is considered to go through chlorination reaction with limited HCl(g) formed as product from the sulfation of KCl(g). K_2SO_4(g) formed as a result of sulfation reactions may deposit on ash particles and react with limited alumina silicates in ash to form high melting temperature potassium alumina silicates. However, formation of potassium alumina silicates is limited by low content of alumina silicates in olive residue ash. Therefore, any unreacted KCl(g) and KOH(g) may condense and deposit on fly ash which forms deposits on furnace wall and heating surfaces (<600˚C) resulting in alkali induced slagging and fouling problems in combustion systems [15,37,56].

When kaolin is added to olive residue, it first forms meta-kaolinite which captures KCl(g) and KOH(g) to form kalsilite ($KAlSiO_4$(s)) and leucite ($KAlSi_2O_6$(s)) minerals with melting temperature of 1600˚C and 1500˚C, respectively. Moreover, through these reactions, kaolin also suppresses the release of KCl(g) and KOH(g) and eliminate alkali induced slagging, silicate melt induced slagging (ash sintering), fouling problems. Capture of KCl(g) and KOH(g) by kaolin to form potassium alumina silicates also results in increase in HCl(g) and SO_2(g) concentrations in the gas phase. This is also verified by the increase of these gases observed in formation profiles with kaolin addition.

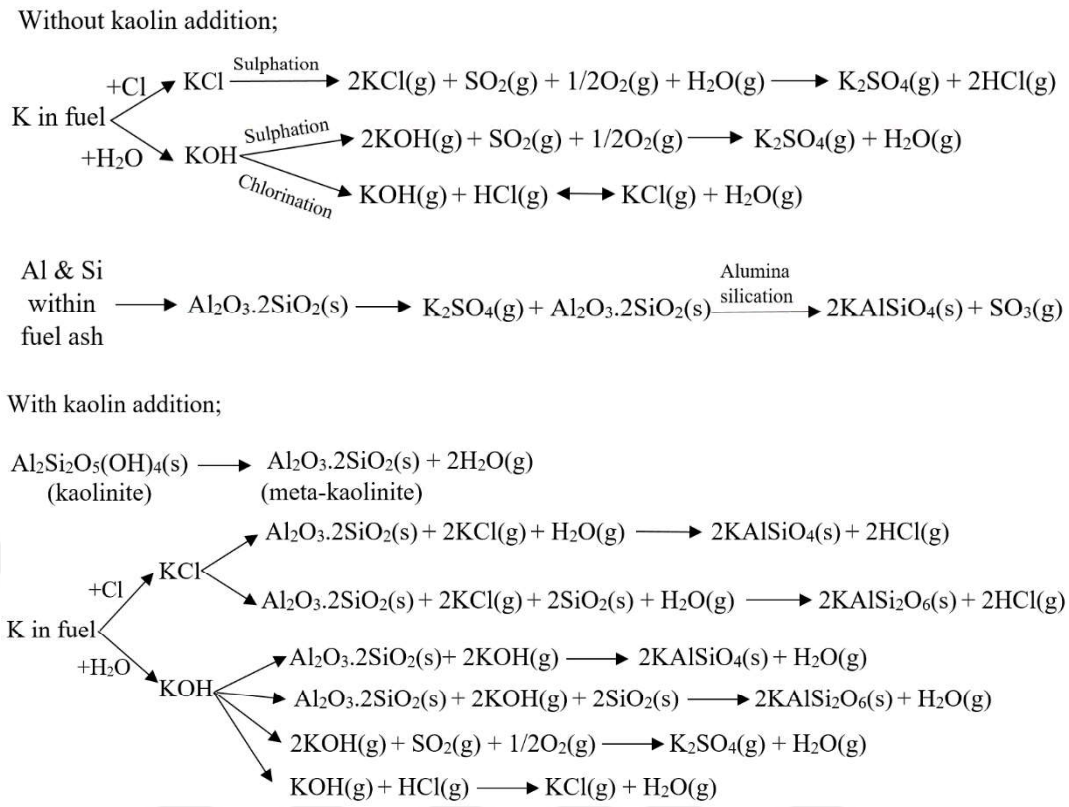

Figure 5.3 Pathway of potassium during combustion of olive residue with kaolin addition [15,33,46,47,53,56,58,62]

In order to verify the results of analyses of gaseous species by TGA-FTIR analyses, analyses of solid samples were also performed. In the following sections, results of the analyses on solid samples are presented and discussed.

5.3. Sintering Tests

In order to visually observe the effect of kaolin addition on ash sintering characteristics of olive residue, olive residue and olive residue-kaolin mixtures were burned at 900˚C in a preheated laboratory furnace. Sintering degree of ashes were determined according to evaluation criteria defined in Chapter 4.

As can be seen from Figure 5.4, according to visual observations, slightly sintering with an easily broken fragile structure is observed in olive residue ash without kaolin addition.

Figure 5.4 Photographs of olive residue ash

Photographs of ash mixture of olive residue with 2% kaolin are illustrated in Figure 5.5. With 2% kaolin addition, slight sintering is observed on parts of the ash mixture. Therefore, sintering degree of the residue is considered to be between slightly sintered and loose ash. The formation of low melting temperature potassium silicates is considered to be due to the fact that the amount of kaolin introduced by 2% addition is not enough to capture all available potassium and convert them to potassium alumina silicates.

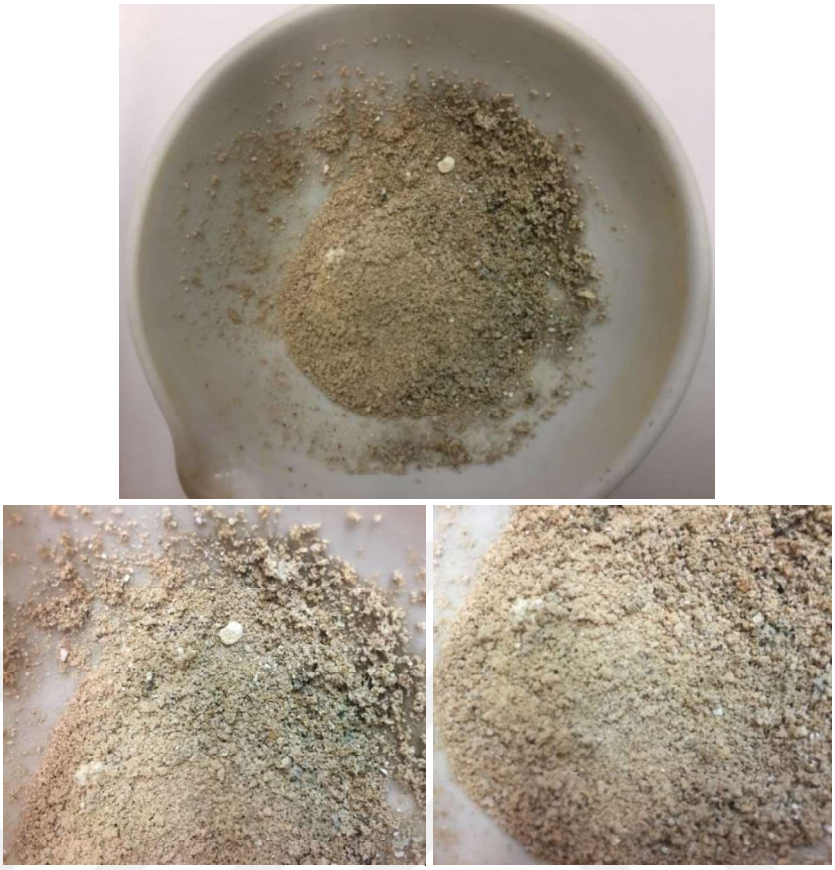

Figure 5.5 Photographs of olive residue + 2% kaolin mixture ash

Photographs of ash mixture of olive residue with 4 and 8% kaolin are presented in Figure 5.6. With 4% kaolin addition, sintering degree decreases from slightly sinter to loose ash while no further improvement is observed with 8% kaolin addition. The photos show that 4% kaolin addition is enough to alleviate the sintering problem.

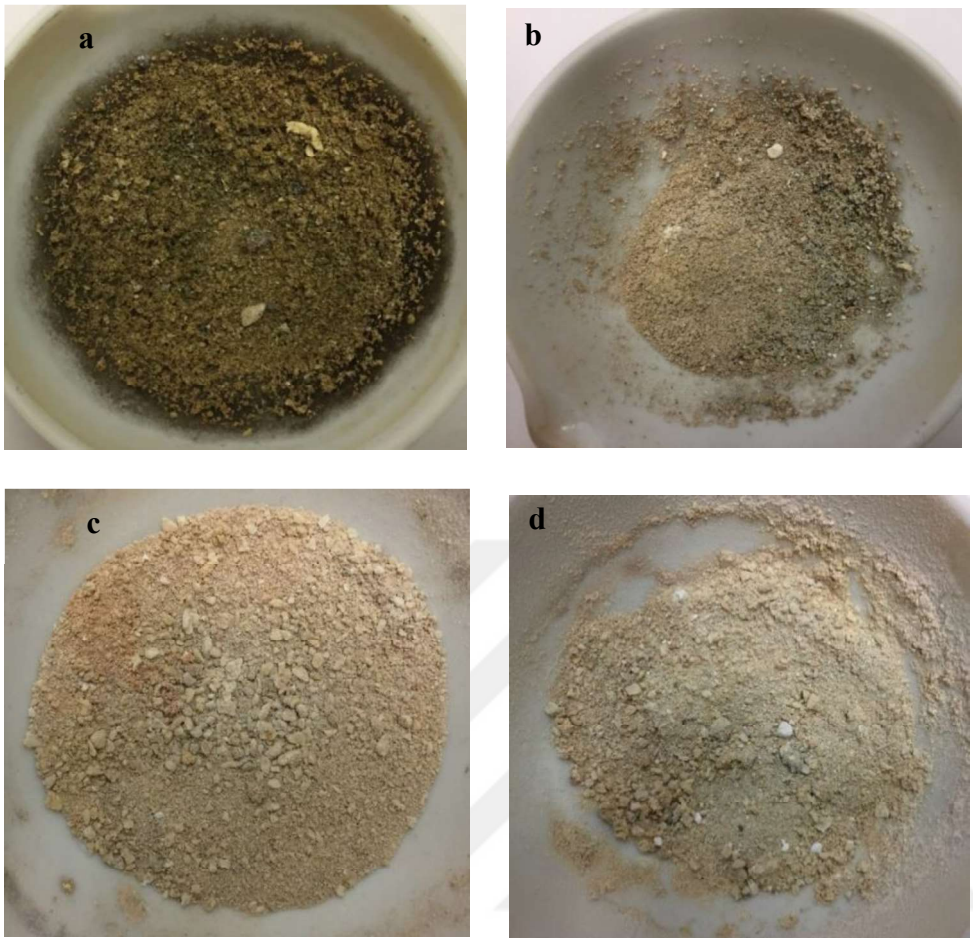

Figure 5.6 Photographs of ashes of olive residue (a), olive residue + 2% (b), 4% (c), 8% (d) kaolin mixtures after sintering tests

5.4. XRF Analyses of Ashes of Olive Residue and Olive Residue-Kaolin Mixtures

XRF analyses were carried out to determine composition of elements in ashes of olive residue and olive residue-kaolin mixtures and results are tabulated in Table 5.2.

Table 5.2 XRF analysis results of ashes of olive residue (OR) and olive residue-kaolin mixtures

Oxide	OR ash	OR+2% kaolin mixture ash	OR+4% kaolin mixture ash	OR+8% kaolin mixture ash
SiO_2	19.9	25.1	31.8	36.3
Al_2O_3	4.47	18.3	24.9	28.7
Fe_2O_3	6.54	3.45	2.26	1.91
CaO	29.6	23.5	15.0	12.9
MgO	4.53	3.55	2.51	2.52
Na_2O	2.25	1.18	0.720	0.542
K_2O	23.1	16.0	16.7	10.8
SO_3	2.36	2.05	1.07	1.05
TiO_2	0.458	0.582	0.695	0.811
P_2O_5	6.58	5.87	4.13	4.27
Cl	0.132	0.284	0.238	0.221

As mentioned above, KCl(g) and KOH(g) are released during combustion of olive residue. In case of kaolin addition, these species are adsorbed on the surface of the meta-kaolinite and react to the crystalline products, potassium alumina silicate minerals, which are retained within the ash. Therefore, potassium retention in the ash of olive residue is expected to increase with increasing kaolin ratio. However, the expected increase in the potassium retention cannot be observed in XRF analysis results due to increase in Al and Si elements added through kaolin in the samples analyzed. Therefore, in order to see the effect of kaolin on potassium retention, wt % of species were re-calculated after subtracting the species added from kaolin. The results are shown in Table 5.3. As can be seen from the table, potassium retention in ash increases with kaolin addition, as also illustrated in Figure 5.7. As can be seen from the figure, no further improvement in potassium retention is observed after 4% kaolin addition.

Table 5.3 Content of olive residue ash and olive residue ash in kaolin mixtures

Oxide	OR ash	OR ash in 2% kaolin mixture	OR ash in 4% kaolin mixture	OR ash in 8% kaolin mixture
SiO_2	19.90	10.11	10.13	1.60
Al_2O_3	4.47	5.33	6.97	0.13
Fe_2O_3	6.54	4.98	3.95	4.63
CaO	29.60	35.65	29.37	37.68
MgO	4.53	5.41	4.97	7.50
Na_2O	2.25	1.80	1.42	1.59
K_2O	23.10	23.92	32.20	30.32
SO_3	2.36	3.00	1.87	2.63
TiO_2	0.46	0.41	0.47	0.59
P_2O_5	6.58	8.96	8.20	12.74
Cl	0.13	0.43	0.47	0.66

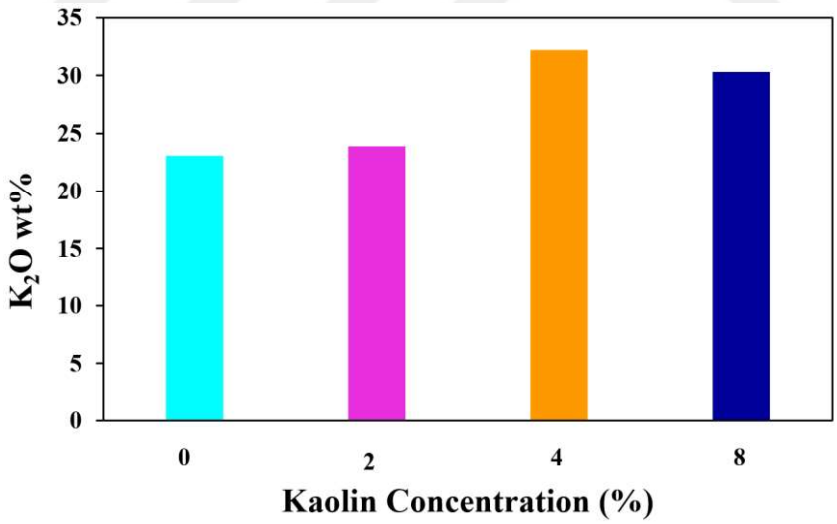

Figure 5.7 Potassium retention within the ash with and without kaolin addition

5.4.1. Evaluation of Fuel Indices

In order to observe effect of kaolin addition on fouling and slagging tendency of olive residue, indices of ashes of olive residue and olive residue-kaolin mixtures were calculated based on XRF analysis results and tabulated in Table 5.4.

Table 5.4 Base to acid ratio and alkali indices of ashes of olive residue (OR) and olive residue-kaolin mixtures

	OR	**OR+2% Kaolin**	**OR+4% Kaolin**	**OR+8% Kaolin**
Base to Acid Ratio	2.92	1.22	0.72	0.50
Alkali Indices				
$\frac{F_{ash} \times (F_{K_2O} + F_{Na_2O})}{GCV}$	0.64	0.44	0.44	0.29
$\frac{\%K_2O + \%Na_2O}{\%SiO_2}$	1.27	0.68	0.55	0.31

According to results of fuel indices, fouling and slagging problems are expected to occur during combustion of olive residue. With kaolin addition, the indices decrease below slagging and fouling tendency limits confirming alleviation of these problems by kaolin addition.

5.4.2. Predicting Ash Melting Temperature from Ternary Phase Diagram

Multicomponent phase diagrams have been proposed as an effective tool to predict ash fusion characteristics (AFC) of an ash with a given composition. Phase diagram allow rapid assessment of the AFC of a particular fuel in comparison with duplicate AFC experiments. According to recent researches on the basis of the ash properties of 30 biomasses burned in operating power plants, initial deformation temperature can be used as the evaluation index for silicate melt-induced slagging [24].

Using ternary phase diagrams, it is possible to predict the effect of additives on melting temperature of biomass ashes based on ash compositions. In ternary phase diagrams,

Gibbs triangle is used which helps to investigate properties of systems composed of three components. It uses the fact that the sum of relative representation of all three components is 100%. The mixture of any composition is displayed with a point inside the equal sided triangle. The concentrations of all three components are shown in mass percentage. The relative amount for compounds are formed on the basis of relative relations [25];

$$P_{SiO_2} = \frac{\%SiO_2}{\%SiO_2+\%Al_2O_3+\%K_2O} \tag{5.1}$$

$$P_{K_2O} = \frac{\%K_2O}{\%SiO_2+\%Al_2O_3+\%K_2O} \tag{5.2}$$

$$P_{Al_2O_3} = \frac{\%Al_2O_3}{\%SiO_2+\%Al_2O_3+\%K_2O} \tag{5.3}$$

In this study, XRF analyses results of ashes of olive residue and olive residue-kaolin mixtures are used to predict effect of kaolin addition on initial deformation temperature of olive residue ash using K_2O-SiO_2-Al_2O_3 ternary phase diagram as the main change is observed in these compounds with kaolin addition. The relative amount of K_2O, SiO_2 and Al_2O_3 in the ashes of olive residue and olive residue-kaolin mixtures, which are calculated based on XRF analyses, are shown in Table 5.5. Ternary phase diagrams developed by using these values are illustrated in Figure 5.8. Moreover, initial deformation temperature of ashes were predicted from ternary phase diagram are tabulated in Table 5.6.

Table 5.5 Relative amount of K_2O, SiO_2 and Al_2O_3 in the ashes of olive residue (OR) and olive residue-kaolin mixtures

	OR ash	**OR+2% kaolin mixture ash**	**OR+4% kaolin mixture ash**	**OR+8% kaolin mixture ash**
P_{K_2O} (%)	49	27	23	14
P_{SiO_2} (%)	42	42	43	48
$P_{Al_2O_3}$ (%)	9	31	34	38

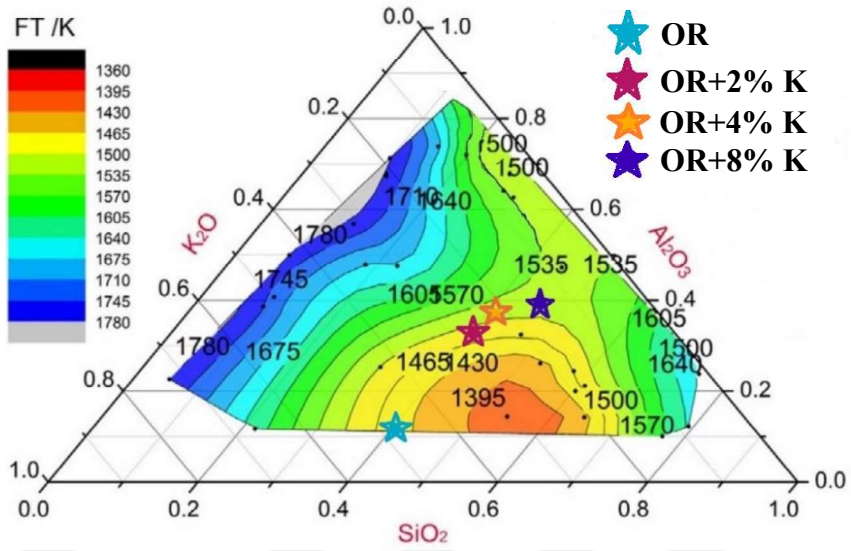

Figure 5.8 K_2O-SiO_2-Al_2O_3 ternary phase diagram [66]

Table 5.6 Predicted initial deformation temperature (IT) interval of olive residue and olive-residue kaolin mixtures

	Predicted IT interval (˚C)
Olive residue ash	1157-1192
OR+2% kaolin mixture ash	1192-1227
OR+4% kaolin mixture ash	1227-1262
OR+8% kaolin mixture ash	1227-1262

As can be seen from Table 5.5, olive residue ash has high relative content of sum of K_2O and SiO_2 (> 90%), and therefore high (SiO_2 + K_2O)/Al_2O_3 ratio which leads to low initial deformation temperature. With kaolin addition, Al_2O_3 content significantly increases which results in a shift to higher temperature region. From 2% to 4% kaolin addition, initial deformation temperature increases while no further increase is observed with 8% kaolin addition which is considered to be due to introducing excess amount of kaolin to the system.

5.5. Determination of Ash Fusion Temperatures

The optimum kaolin ratio for elimination of ash sintering in olive residue combustion was determined as 4% in Sections 5.3 and 5.4. Therefore, to confirm these results, initial deformation temperature (IT), softening temperature (ST), hemispherical temperature (HT) and fluid temperature (FT) of olive residue and olive residue + 4% kaolin mixture were also determined based on ASTM 1857 - Standard Test Method for Fusibility of Coal and Coke Ash. Pictures of olive residue and olive residue + 4% kaolin mixture samples during ash fusibility test are illustrated in Figure 5.9 and 5.10, respectively. Furthermore, ash fusion temperatures are tabulated in Table 5.7.

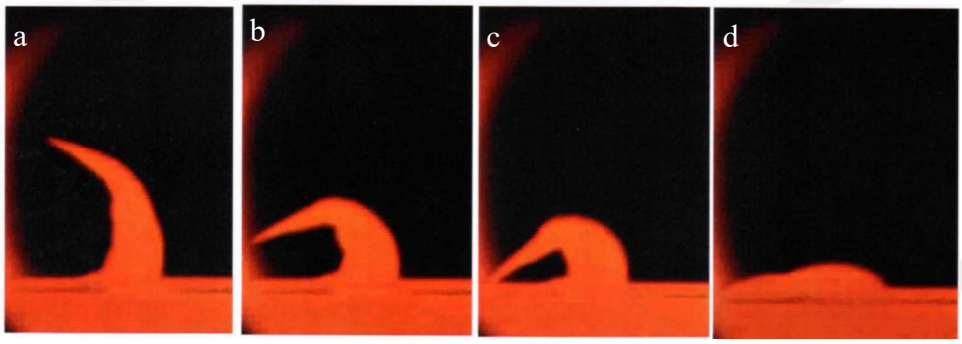

Figure 5.9 Picture of olive residue ash sample during ash fusion test

(a: IT, B: ST, c: HT, d: FT)

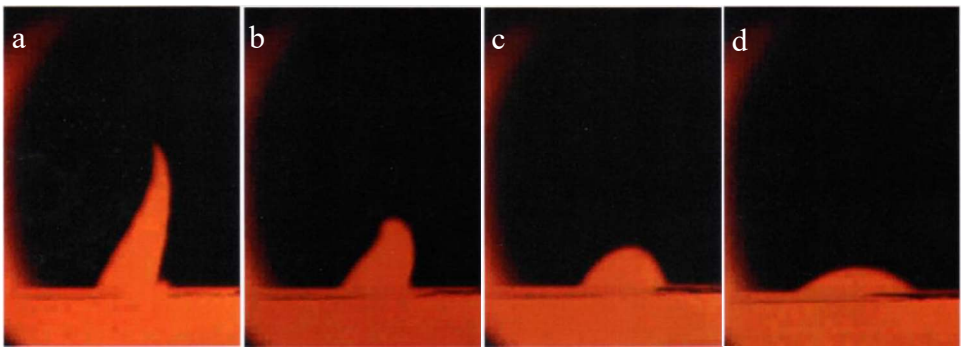

Figure 5.10 Picture of olive residue + 4% kaolin mixture ash sample during ash fusion test

(a: IT, B: ST, c: HT, d: FT)

Table 5.7 Ash fusion temperatures of olive residue (OR) and olive residue + 4% kaolin mixture

	IT (˚C)	ST (˚C)	HT (˚C)	FT (˚C)
OR	1126	1131	1140	1166
OR+4% Kaolin	1332	1358	1372	1410

As can be seen in Table 5.7, kaolin addition increases critical ash fusion temperatures of olive residue about 200˚C which is consistent with literature [16,25].

Ash melting temperatures of olive residue and olive residue-kaolin mixtures predicted from K_2O-SiO_2-Al_2O_3 ternary phase diagram in Section 5.4 are compared with experimentally measured initial deformation temperature (IT) which is considered more critical than the other temperatures, since the ash becomes sticky due to partial melting and may initiate sintering at this temperature [16]. For olive residue ash, results are close while for the ash of olive residue + 4% kaolin mixture, higher predicted temperature is observed. Therefore, ternary phase diagrams can be used to predict initial deformation temperature and to observe effect of additives on ash melting temperature of biomasses; however, ash fusion tests should be applied to obtain more accurate results.

5.6. XRD Analysis of Ashes of Olive Residue and Olive Residue-Kaolin Mixtures

XRD analysis of kaolin was performed and the pattern is shown in Figure 5.11. Kaolinite crystal, which is the most common mineral within the kaolin, is the dominant crystalline observed in XRD pattern which is consistent with the findings of [56].

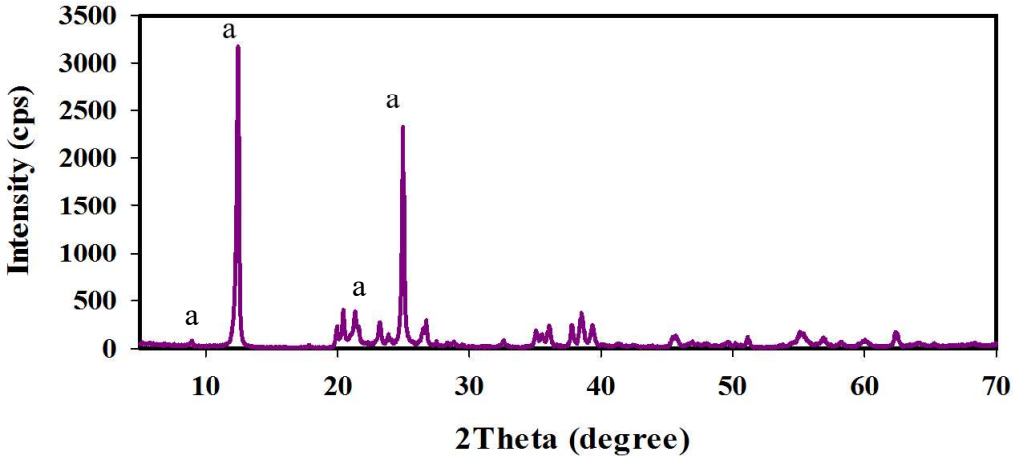

Figure 5.11 XRD pattern of kaolin (a: kaolinite)

XRD ash analysis of olive residue and olive residue-kaolin mixtures were also conducted in order to identify the mineral phase compounds formed by the interaction between kaolin and potassium in olive residue. As illustrated in Figure 5.12, the structure of olive residue ash is mainly amorphous with small peaks of kalsilite and huntite crystals. With kaolin addition, the intensity of kalsilite crystalline significantly increases. However, with 8% kaolin addition, kalsilite peak intensity dramatically decreases while that of quartz crystal becomes dominant. This is considered to be due to presence of abundant amount of kaolin which is more than required amount to capture available potassium. Although potassium with meta-kaolinite reaction can produce both kalsilite and leucite crystals, only kalsilite is observed in XRD pattern. This is considered to be due to the fact that the molar ratio of Si to Al is 1 for kalsilite and 2 for leucite indicating that kalsilite formation is more favourable which is in agreement with the finding of [17].

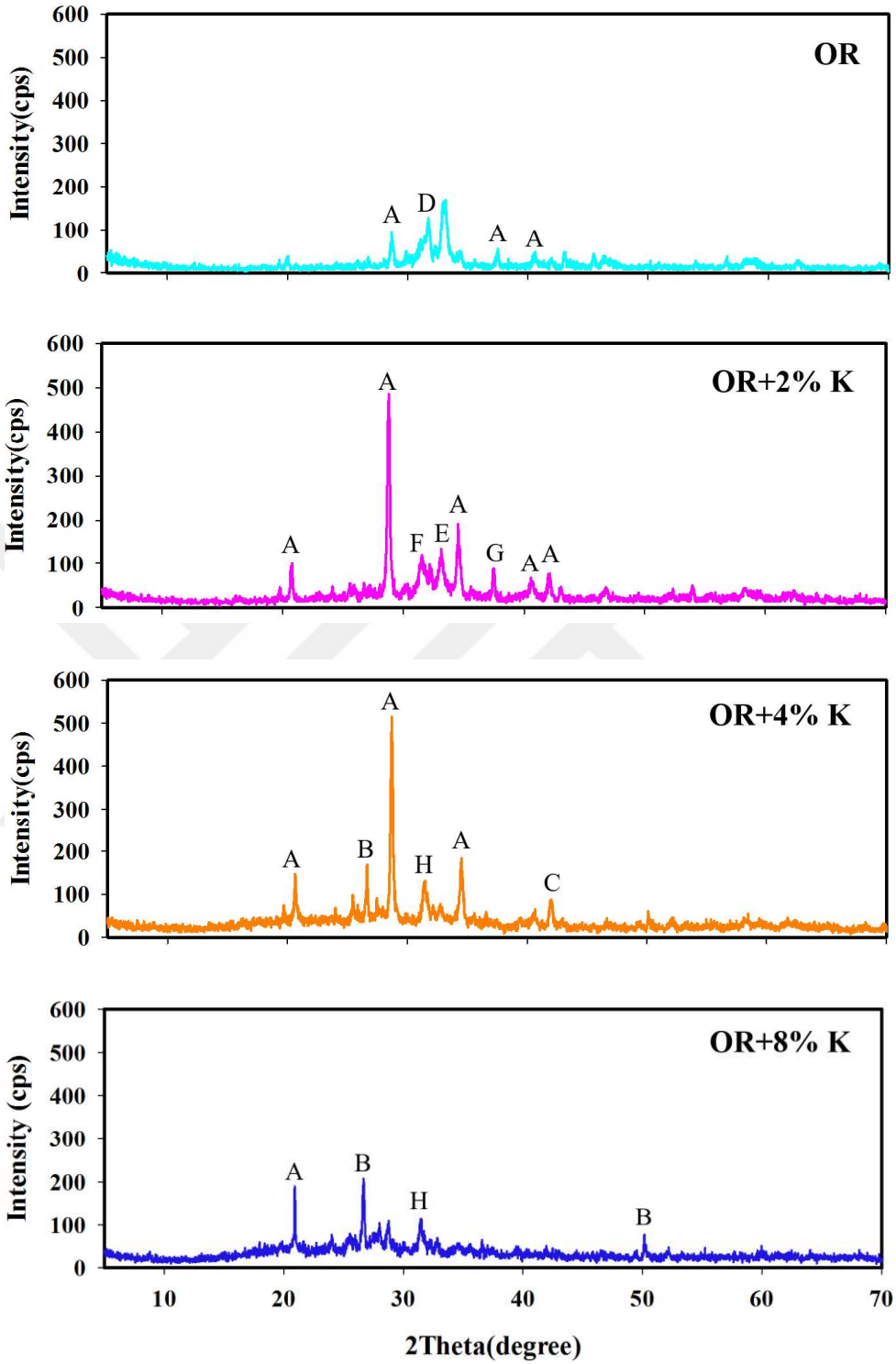

Figure 5.12 XRD pattern of olive residue olive residue-kaolin mixture ashes

(A: Kalsilite ($KAlSiO_4$), B: Quartz (SiO_2), C: Calcite ($CaCO_3$), D: Huntite ($Mg_3Ca(CO_3)_4$, E: Marcasite (FeS_2), F: Anhydrite ($CaSO_4$), G: Pyrite (FeS_2), H: Hydroxylapatite ($Ca_5(PO_4)_3(OH)$))

CHAPTER 6

CONCLUSIONS

6.1. General

In this thesis study, effect of kaolin addition on combustion characteristic of olive residue was investigated by using TGA combined with FTIR spectrometer in parallel with ash characteristics by XRF and XRD. The following conclusions were reached under the observations of this study:

- Addition of kaolin does not significantly affect combustion of olive residue. However, rate of weight loss during char combustion decreases with increasing kaolin addition.
- CO_2(g) emission does not change with kaolin addition while CO(g) emission increases due to decrease in burning quality.
- Capture of KCl(g) and KOH(g) by kaolin to form potassium alumina silicates results in increase in HCl(g) and SO_2(g) concentrations in the gas phase.
- Sintering degree of olive residue ash decreases from slightly sinter to loose ash with 4% kaolin addition while no further improvement is observed with 8% kaolin addition.
- Potassium retention in ash increases up to 4% kaolin addition forming mainly kalsilite crystals. No significant improvement in potassium retention is observed with further addition of kaolin due to abundant amount of Al and Si introduced via kaolin.
- Ash fusion temperatures (IT, ST, HT, FT) are increased by about 200˚C with 4% kaolin addition.

- Optimum 4% kaolin addition decreases fouling and slagging tendency of olive residue during combustion.

6.2. Suggestions for Future Work

Based on the experience gained in the present study, the main recommendation for future extension of the work would be to conduct combustion tests burning olive residue with kaolin addition in a pilot scale FBC system.

REFERENCES

[1] BP Statistical Review of World Energy June 2016, Retrieved 15 April 2017 from http://www.bp.com/statisticalreview.

[2] Sami M., Annamalai K., Wooldridge M., "Co-firing of Coal and Biomass Fuel Blends", *Progress in Energy and Combustion Science*, vol. 27, pp. 171- 214, 2001.

[3] Key World Energy Statistics 2016, Retrieved 4 April 2017 from https://www.iea.org/publications/freepublications/publication/key-world-energy-statistics.html.

[4] International Energy Outlook 2016, Retrieved 15 April 2017 from https://www.eia.gov/outlooks/ieo/world.php.

[5] Khan, A.A., de Jong, W., Jansens, P.J., Spliethoff, H. "Biomass Combustion in Fluidized Bed Boilers: Potential Problems and Remedies", *Fuel Processing Technology*, vol. 90, pp. 21-50, 2009.

[6] Ots, A. "Thermophysical Properties of Ash Deposit on Boiler Heat Exchanger Surfaces", *in Proceedings of International Conference on Heat Exchanger Fouling and Cleaning*, Crete Island, Greece, June 05-10, pp. 150-166, 2011.

[7] Baxter L., Koppejan J., "Biomass-Coal Co-combustion: Opportunity for Affordable Renewable Energy", *Euro Heat & Power*, vol. 1, pp. 1286-1302, 2004.

[8] Cammarota, A., Chirone, R., Scala, F., "Bed Agglomeration during Fluidized Bed Combustion of Olive Husk", *in Proceedings of 18th International Conference on Fluidized Bed Combustion* (Ed. Jia L.), FBC2005-098 in CD-ROM, ASME, Toronto, Ontario, Canada, May 22-25, 2005.

[9] Hughes E.E., Tillman D.A., "Biomass Co-firing: Status and Prospects 1996", Fuel Processing Technology, vol. 54, pp. 127-142, 1998.

[10] Guanyi C., Mengxiang F., Zhongyang L., Xuantian L., Zhenglun S., Kefa C., Mingjiang N., Experimental Research on Rice Husk Combustion in CFB Boiler and The Design of a 35 T/H Rice Husk Fired CFB Boiler, *in Proceedings of 14th International Conference on Fluidized Bed Combustion* (Ed. Preto F.D.S.), vol. 1, 175-181, ASME, Vancouver, Canada, May 11-14, 1997.

[11] Chaivatamaset, P., Sricharoon, P., Tia, S., "Bed Agglomeration Characteristics of Palm Shell and Corncob Combustion in Fluidized Bed", *Applied Thermal Engineering*, vol. 31, pp. 2916-2927, 2011.

[12] Skrifvars, B.J., Backman, R., Hupa, M., Sfiris, G., Abyhammar, T., Lyngfelt, A. "Ash Behaviour in a CFB Boiler during Combustion of Coal, Peat or Wood", *Fuel*, vol. 77, pp. 65-70, 1998.

[13] Öhman, M., Nordin, A. "Bed Agglomeration Characteristics during Fluidized Bed Combustion of Biomass Fuels", *Energy & Fuels*, vol. 14, pp. 169-178, 2000.

[14] Boström, D., Grimm, A., Boman, C., Björrnbom, E. "Influence of Kaolin and Calcite Additives on Ash Transformations in Small Scale Combustion of Oat", *Energy & Fuels*, vol. 23, pp. 5184-5190, 2009.

[15] Steenari, B. M.; Lundberg, A.; Pettersson, H.; Wilewska-Bien, M.; Andersson, D., "Investigation of Ash Sintering during Combustion of Agricultural Residues and the Effect of Additives", *Energy & Fuels*, vol. 23, pp. 5655-5662, 2009.

[16] Wang, L., Skjevrak, G., Hustad, J., Gronli, M., Skreiberg, Ø. "Effects of Additives on Barley Straw and Husk Ashes Sintering Characteristics", *Energy Procedia*, vol.20, pp. 30-39, 2012.

[17] Glazer, M.P., *Alkali Metals in Combustion of Biomass with Coal*, M.Sc. Thesis, Poznan University of Technology, Poznań, 2006.

[18] Hansen, L. A., Frandsen, F. J., Dam-Johansen, K., Sorensen H. S., Skrifvars, B. J., "Characterization of Ashes and Deposits from High-Temperature Coal-Straw Co-firing", *Energy and Fuels*, vol. 13, pp. 803-816, 1999.

[19] Biomass Co-firing in Coal Power Plants (n.d.) Retrieved 26 June 2017 from https://ieaetsap.org/ETechDS/PDF/E21IR_Biocofiring_PL_Jan2013_final_GSOK.pdf.,

[20] Wu, H., Castro, M., Jensen, P.A., Frandsen, F.J., Glarborg, P., Dam-Johansen K., Røkke, M., Lundtorp, K., "Release and Transformation of Inorganic Elements in Combustion of a High Phosphorus Fuel", *Energy Fuels*, vol. 25, pp. 2874–86, 2011.

[21] Tchoffor, P., Davidsson, K., Thunman, H., "Effects of Steam on the Release of Potassium, Chlorine, and Sulfur during Char Conversion, Investigated under Dual-Fluidized-Bed Gasification Conditions", *Energy & Fuels*, vol. 28, pp. 6953-6965, 2014.

[22] Wang, L., Becidan, M., Skreiberg, Ø., "Testing of zeolite and kaolin for preventing ash sintering and fouling during biomass combustion'', *Chemical Engineering Transactions*, vol. 35, pp. 1159-1164, 2013.

[23] Fournel, S., Palacios, J.H., Godbout, S., Heitz, M., "Effect of additives and fuel blending on emissions and ash-related problems from small-scale combustion of reed canary grass", *Agriculture*, vol. 5, pp. 561-576, 2015.

[24] Llorente, M.J., Arocas, P.D., Nebot, L.G., Garcia, J.E., "The Effect of Addition of Chemical Materials on the Sintering of Biomass Ash", *Fuel*, vol. 87, pp. 2651-2658, 2008.

[25] Jandacka, J., Malcho, M., Ochodek, T., Kolonicny, J., Holubcik, M., "The Increase of Silver Grass Ash Melting Temperature Using Additives", *International Journal of Renewable Energy Research*, vol. 5, pp. 258-265, 2015.

[26] Turkey in Statistics 2014, Turkish Statistical Institute, Printing Division, Ankara, 2015.

[27] Zhu, J., "Ash deposition in biomass combustion or co-firing for power/heat generation", *Energies*, vol. 5, pp. 5171-5189, 2012.

[28] Easterly J.L., Burnham M., "Overview of Biomass and Waste Fuel Resources for Power Production", *Biomass and Bioenergy*, vol. 10, pp. 79-92, 1996.

[29] Gogebakan, Z., "Co-firing Biomass with Coal in Bubbling Fluidized Bed Combustors". PhD Thesis. Middle East Technical University, 2007.

[30] Vamvuka, D., Bandelis, G., "Evaluation of Wood Residues from Crete as Alternative Fuels", *International Journal of Energy and Environment*, vol. 1, pp. 667-674, 2010.

[31] Wei, X., Schnell U., Hein KRG., "Behaviour of Gaseous Chlorine and Alkali Metals during Biomass Thermal Utilization", *Fuel*, vol. 84, pp. 841–848, 2005.

[32] Niu, Y.Q., Tan, H.Z., Wang, X.B., Liu, Z.N., Liu, Y., Xu, T.M., "Study on deposits on the surface, upstream, and downstream of bag filters in a 12 MW biomass-fired boiler", *Energy Fuel*, vol. 24, pp. 2127–32, 2010.

[33] Niu, YQ., Tan, H., Hui, S., "Ash-related Issues During Biomass Combustion: Alkali-Induced Slagging, Silicate Melt-Induced Slagging (Ash Fusion), Agglomeration, Corrosion, Ash Utilization, and Related Countermeasures", *Progress in Energy and Combustion Science*, vol. 52, pp. 1-61, 2016.

[34] Niu Y, Zhu Y, Tan H, Hui S, Jing Z, Xu W., "Investigations on Biomass Slagging in Utility Boiler: Criterion Numbers and Slagging Growth Mechanisms", *Fuel Process Technology*, vol. 128, pp. 499–508, 2014.

[35] Werther J., Saenger M., Hartge E.U., Ogada T., Siagi Z., "Combustion of Agricultural Residues", *Progress in Energy and Combustion Science*, vol. 26, pp. 1-27, 2000.

[36] Bapat, D.W, Kulkarni, S.V., Bhandarkar, V. P., "Design and Operating Experience on Fluidized Bed Boiler Burning Biomass Fuels with High

Alkaline Ash", *in Proceedings of 14th International Conference on Fluidized Bed Combustion* (Ed. Preto F.D.S.), vol. 1, pp. 165-174, ASME, Vancouver, Canada, May 11-14, 1997.

[37] Brus, E., Öhman, M., Nordin, A., "Mechanisms of Bed Agglomeration during Fluidized-Bed Combustion of Biomass Fuels", *Energy & Fuels*, vol. 19, pp. 825-832, 2005.

[38] Kim, M., Lee, J., "Prevention of Bed Agglomeration with Iron Oxide during Fluidized Bed Incineration of Refuse-Derived Fuels", *Korean Journal of Chemical Engineering*, vol. 26, pp. 1399-1404, 2009.

[39] Capareda, S. C., "Introduction to Biomass Energy Conversions", Boca Raton: CRC Press/Taylor & Francis Group, 2014.

[40] Basu, P., "Circulating Fluidized Bed Boilers", Springer, Switzerland, 2016.

[41] Nunes, L.J.R., Matias, J.C.O., Catalao, J.P.S., "Biomass Combustion Systems: A Review on the Physical and Chemical Properties of the Ashes", *Renewable and Sustainable Energy Reviews*, vol. 53, pp. 235-242, 2016.

[42] Gudka, B., Jones, J.M., Lea-Langton A.R., Williams, A., Saddawi, A., "A Review of the Mitigation of Deposition and Emission Problems during Biomass Combustion Through Washing Pre-Treatment", Journal of the Energy Institute, vol. 89, pp. 159-171, 2016.

[43] Wang, L., Hustad, J.E., Skreiberg, Ø., Skjevrak, G., Grønli, M., "A Critical Review on Additives to Reduce Ash Related Operation Problems in Biomass Combustion Applications", *Energy Procedia*, vol.20., pp. 20-29, 2012.

[44] Wang, L., Becidan, M., Skreiberg, Ø., "Sintering Behavior of Agricultural Residues Ashes and Effects of Additives", *Energy & Fuels*, vol. 26, pp. 5917-5929, 2012.

[45] Wang, L., Skreiberg, Ø., Becidan, M., Li, H., "Investigation of Rye Straw Ash Sintering Characteristics and the Effect of Additives", *Applied Energy*, vol. 162, pp. 1195-1204, 2016.

[46] Tran K., Lisa, K., Steenari, B., Lindqvist, O. "A Kinetic Study of Gaseous Alkali Capture by Kaolin in the Fixed Bed Reactor Equipped with an Alkali Detector", *Fuel*, vol.84, pp. 169-175, 2005.

[47] Boman, C.; Böström, D.; Öhman, M. Effect of fuel additive sorbent (kaolin and calcite) on aerosol particle emission and characteristics during combustion of pelletized woody biomass. *Proceedings of the 16th European Biomass Conference & Exhibition 2008*, Valencia, Spain; EU BC&E: Florence, Italy, June 2008; pp 1514−1517.

[48] Wang, L., Becidan, M., Skreiberg, Ø., "Testing of zeolite and kaolin for preventing ash sintering and fouling during biomass combustion", *Chemical Engineering Transactions*, vol. 35, pp. 1159-1164, 2013.

[49] Garba, M.U., Ingham, D.B., Ma, L., Porter, R.T.J., Pourkashnian, M., Tan, H.Z., Willams, A., "Prediction of Potassium Chloride Sulfation and Its Effect on Deposition in Biomass-Fired Boilers", *Energy&Fuels*, vol. 26, pp. 6501-6508, 2012.

[50] Blomberg, T., "A Thermodynamic Study of the Gaseous Potassium Chemistry in the Convection Sections of Biomass Fired Boilers", *Materials and Corrosion*, vol. 62, pp. 635-641, 2011.

[51] Dayton D.C., Milne T.A. "Laboratory Measurements of Alkali Metal Containing Vapors Released during Biomass Combustion", In: Baxter L., DeSollar R. (eds) *Applications of Advanced Technology to Ash-Related Problems in Boilers*. Springer, Boston, MA, 1996.

[52] Iisa, K., Lu, Y., "Sulfation of Potassium Chloride at Combustion Conditions", *Energy & Fuels*, vol. 13, pp. 1184-1190, 1999.

[53] Broström, B., "Aspects of Alkali Chloride Chemistry on Deposit Formation and High Temperature Corrosion in Biomass and Waste Fired Boilers", *Energy Technology and Thermal Process Chemistry*. Umeå University, 2010.

[54] Valmari, T., “Potassium Behavior during Combustion of Wood in Circulating Fluidized Bed Power Plants”, *Espoo 2000*, Technical Research Centre of Finland, VTT Publications 414.

[55] Salmenoja, K., Makela, K., “Prevention of Superheater Corrosion in the Combustion of Biofuels”, *Corrosion 2000*, 2000.

[56] Konsomboon, S., Pipatmanomai, S., Madhiyanon, T., Tia, S. “Effect of Kaolin Addition on Ash Characteristics of Palm Empty Bunch upon Combustion”, *Applied Energy*, vol.88, pp. 298-305, 2011.

[57] Wang, L., Skreiberg, Ø., Becidan, M., “Investigation of Additives for Preventing Ash Fouling and Sintering during Barley Straw Combustion”, *Applied Thermal Energy*, vol. 70, pp. 1262-1269, 2014.

[58] Niu, Y., Wang, Z., Zhu, Y., Zhang, X., Tan, H., Hui, S., “Experimental Evaluation of Additives and K2O-SiO2-Al2O3 Diagrams on High-Temperature Silicate Melt-Induced Slagging During Biomass Combustion”, *Fuel*, vol. 179, pp. 52-59, 2016.

[59] Xiong, S., Burvall, J., Örberg, H., Kalen, G., Thyrel, M., Öhman, M., Boström, D., “Slagging Characteristics during Combustion of Corn Stovers with and without Kaolin and Calcite”, *Energy & Fuels*, vol. 22, pp. 3465-3470, 2008.

[60] Schmitt, V.E.M., Kaltschmitt, M., “Effect of Straw Proportion and Ca- And Al-Containing Additives on Ash Composition and Sintering of Wood–Straw Pellets”, *Fuel*, vol. 109, pp. 551-558, 2013.

[61] Sommersacher, P., Brunner, T., Obernberger, I., Kienzl, N., Kanzian, W., “Application of Novel and Advanced Fuel Characterization Tools for the Combustion Related Characterization of Different Wood/Kaolin and Straw/Kaolin Mixtures”, *Energy & Fuels*, vol.27, pp. 5192-5206, 2013.

[62] Steenari, B. M.; Lindqvist, O., “High-temperature Reactions of Straw Ash and the Anti-Sintering Additives Kaolin and Dolomite”, *Biomass & Bioenergy*, vol.14, pp. 67-76, 1998.

[63] Liao, Y., Wu, S., Chen, T., Cao, Y., Ma, X., "The Alkali Metal Characteristics during Biomass Combustion with Additives", *Energy Procedia*, vol. 75, pp. 124-129, 2015.

[64] Xie, Z., Ma, X., "HCl Emission Characteristics during the Combustion of Eucalyptus Bark", *Energy & Fuels*, vol. 28, pp. 5826-5833, 2014.

[65] Coda, B., Aho, M., Berger, R., Hein, K., "Behavior of Chlorine and Enrichment of Risky Elements in Bubbling Fluidized Bed Combustion of Biomass and Waste Assisted by Additives", *Energy & Fuels*, vol. 15, pp. 680-690, 2001.

[66] Paneru, M., Babat, S., Maier, J., Scheffknecht, G., "Role of Potassium in Deposit Formation during Wood Pellets Formation", *Fuel Processing Technology*, vol. 141, pp. 266-275, 2016.

[67] Madhiyanon, T., Sathitruangsak, P., Sungworagarn, S., Fukuta, S., Tia, S., "Ash and Deposit Characteristics from Oil-Palm Empty-Fruit-Bunch (EFB) Firing with Kaolin Additive in a Pilot-Scale Grate-Fired Combustor", *Fuel Processing Technology*, vol. 115, pp. 182-191, 2013.

[68] Öhman, M., Nordin, A., "The Role of Kaolin in Prevention of Bed Agglomeration during Fluidized Bed Combustion of Biomass Fuels", *Energy & Fuels*, vol. 14, pp. 618-624, 2000.

[69] Davidsson, K.O., Steenari, B.M., Eskilsson, D. K., "Kaolin Addition during Biomass Combustion in a 35 MW Circulating Fluidized-Bed Boiler", *Energy & Fuels*, vol. 21, pp. 1959-1966, 2007.

[70] Davidsson, K.O., Åmand, L.E., Steenari, B.M., Elled, A.L., Eskilsson, D., Leckner, B., "Countermeasures Against Alkali-Related Problems During Combustion of Biomass in a Circulating Fluidized Bed Boiler", *Chemical Engineering Science*, vol. 63, pp. 5314-5329, 2008.

[71] Vamvuka, D., Zografos, D., Alevizos, G., "Control Methods for Mitigating Biomass Ash-Related Problems in Fluidized Beds", *Bioresource Technology*, vol. 99, pp. 3534-3544, 2008.

[72] Morgan, P.A., Robertson, S.D., Unsworth, J.F., "Combustion Studies by Thermogravimetric Analysis: 1. Coal Oxidation", *Fuel*, vol. 65, pp. 1546-1551, 1986.

[73] Pan, Y.P., Gan, Y., Serageldin, M.A., "A Study of Thermal Analytical Values for Coal Blends Burned in an Air Atmosphere", *Thermochimica Acta*, vol. 180, pp. 203-217, 1991.

[74] Arenillas, A., Rubiera, F., Arias, B., Pis, J., Faúndez, J., Gordon, A., García, X., "A TG/DTA Study on the Effect of Coal Blending on Ignition Behaviour", *Journal of Thermal Analysis and Calorimetry*, vol. 76, pp. 603-614, 2004.

[75] Arias, B., Pevida, C., Rubiera, F., Pis, J.J., "Effect of Biomass Blending on Coal Ignition and Burnout during Oxy-Fuel Combustion", *Fuel*, vol. 87, pp. 2753-2759, 2008.

[76] Li, Q., Zhao, C., Chen, X., Wu, W., Li, Y., "Comparison of Pulverized Coal Combustion in Air and in O_2/CO_2 Mixtures by Thermo-Gravimetric Analysis", *Journal of Analytical and Applied Pyrolysis*, vol. 85, pp. 521-528, 2009.

[77] Duan, L., Zhao, C., Zhou, W., Liang, C., Chen, X., "Sulfur Evolution from Coal Combustion in O_2/CO_2 Mixture", *Journal of Analytical and Applied Pyrolysis*, vol. 86, pp. 269-273, 2009.

[78] Charland, J.P., MacPhee, J.A., Giroux, L., Price, J.T., Khan, M.A., "Application of TG-FTIR to the Determination of Oxygen Content of Coals", *Fuel Processing Technology*, vol. 81, p. 211-221, 2003.

[79] Di Nola, G., de Jong, W., Spliethoff, H., "TG-FTIR Characterization of Coal and Biomass Single Fuels and Blends Under Slow Heating Rate Conditions: Partitioning of the Fuel-Bound Nitrogen", *Fuel Processing Technology*, vol. 91, pp. 103-115, 2010.

[80] Kaljuvee, T., Pelt, J., Radin, M., "TG-FTIR Study of Gaseous Compounds Evolved at Thermooxidation of Oil Shale", *Journal of Thermal Analysis and Calorimetry*, vol. 78, pp. 399-414, 2004.

[81] Pitkänen, I., Huttunen, J., Halttunen, H., Vesterinen, R., "Evolved Gas Analysis of Some Solid Fuels by TG-FTIR", *Journal of Thermal Analysis and Calorimetry*, vol. 56, pp. 1253-1259, 1999.

[82] Groenewoud, W.M., de Jong, W., "The Thermogravimetric Analyser - Coupled - Fourier Transform Infrared/Mass Spectrometry Technique", *Thermochimica Acta*, vol. 286, pp. 341-354, 1996.

[83] Yuzbasi, N., "Pyrolysis and Combustion Behaviour of Various Fuels in Oxygen-Enriched Air and CO_2 Atmospheres". MSc Thesis. Middle East Technical University, 2011.

[84] Su, S., Pohl, J.H., Holcombe, D., Hart, J. A., "Techniques to Determine Ignition, Flame Stability and Burnout of Blended Coals in P.F. Power Station oilers", *Progress in Energy and Combustion Science*, vol. 27, pp. 75-98, 2001.

[85] Jia, L., Anthony, E.J., Lau, I., Wang, J., "Study of Coal and Coke Ignition in Fluidized Beds", *Fuel*, vol. 85, vol. 635-642, 2006.

APPENDICES

A.1. SEM/EDX Analysis of Ashes of Olive Residue and Olive Residue-Kaolin Mixtures

The morphology and microchemistry of the ashes of olive residue and olive residue-kaolin mixtures were examined by SEM/EDX analysis. Ashes of olive residue and olive residue + 2% and 8% kaolin mixtures were obtained at 900˚C in a preheated laboratory furnace.

SEM images of the all samples in epoxy and a representative SEM image of large and fine olive residue ash particles are shown in Figure A.1. As the SEM image of all samples is investigated, dominance of larger size particles is observed which is considered to be due to occurrence of silicate melt induced slagging of the olive residue ash.

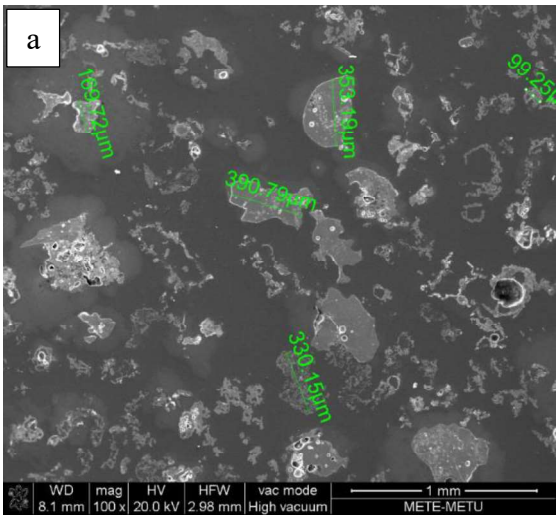

Figure A.1 SEM images of olive residue ash (cont'd)

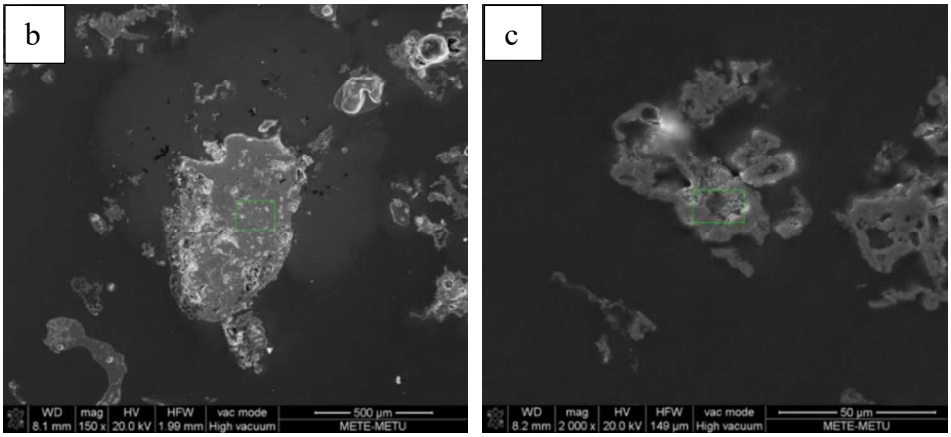

Figure A.1 SEM images of olive residue ash

(a: overall image, b: large ash particle, c: fine ash particle)

For large and fine selected ash particles, EDX area analyses were performed and illustrated in Figure A.2 and Figure A.3, respectively. Large ash particles mainly consist of K, Si and Ca elements indicating presence of low melting temperature potassium silicates which results in ash sintering problems.

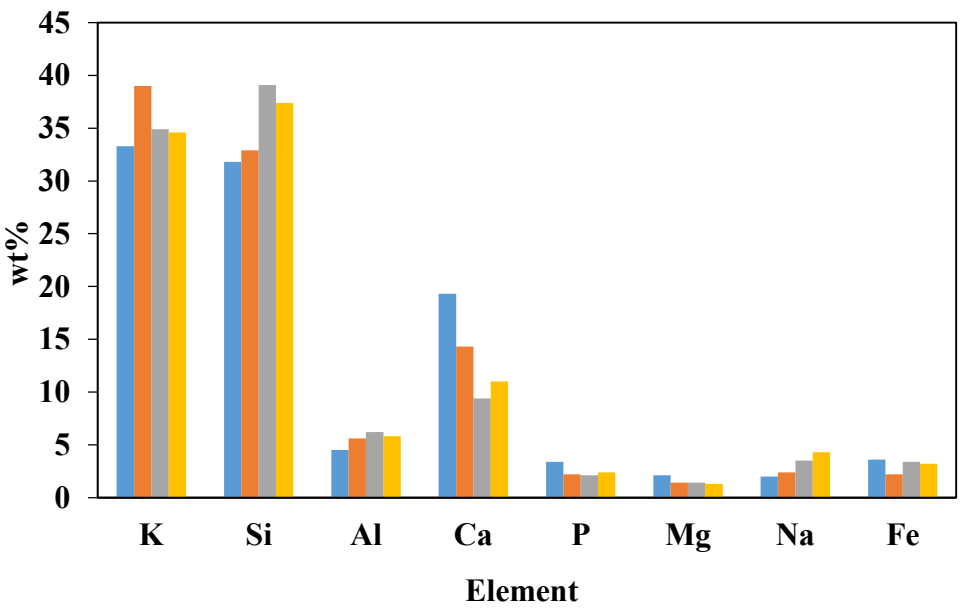

Figure A.2 EDX area analysis of large olive residue ash

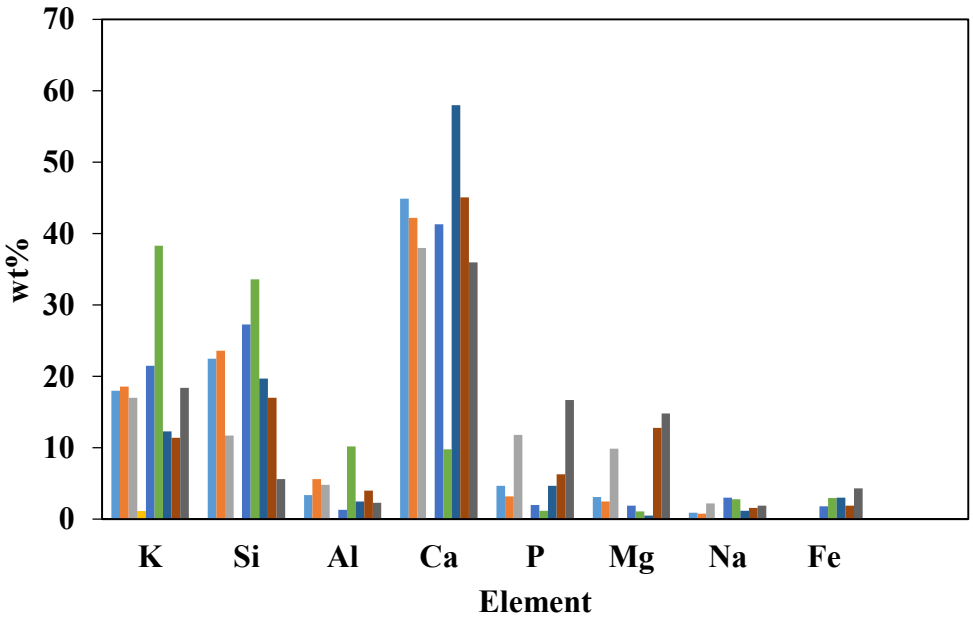

Figure A.3 EDX area analysis of fine olive residue ash samples

SEM images of the all samples in epoxy and a representative SEM image of large and fine olive residue + 2% kaolin mixture ash particles are shown in Figure A.4. The dominance of large particles is still observed with 2% kaolin addition. Moreover, needle like structure of kaolin particles is observed in the SEM images.

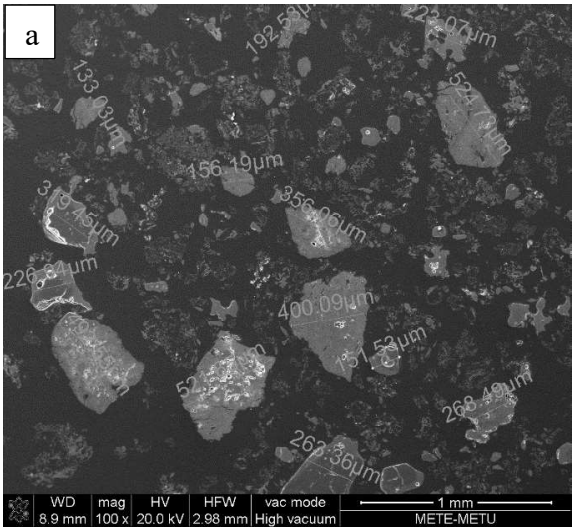

Figure A.4 SEM images of olive residue + 2% kaolin mixture ash (cont'd)

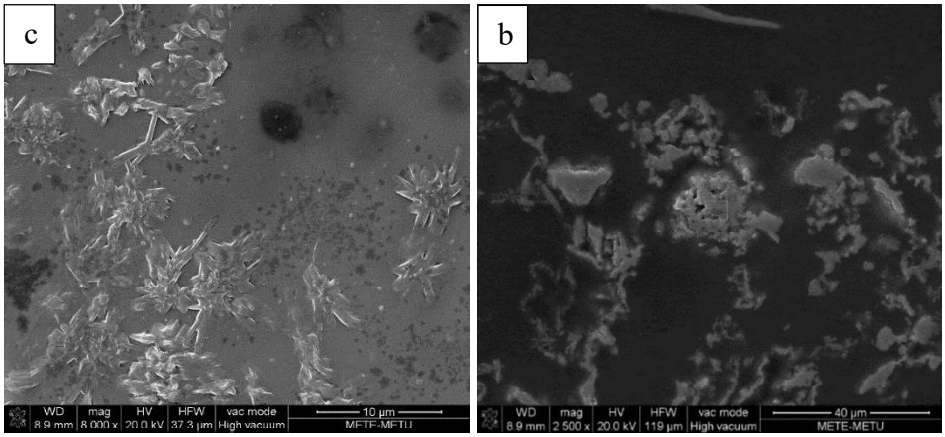

Figure A.4 SEM images of olive residue + 2% kaolin mixture ash
(a: overall image, b: large ash particle, c: fine ash particle)

For large and fine selected ash particles, EDX area analyses were performed and results are illustrated in Figure A.5 and Figure A.6, respectively. According to EDX area analysis, K, Si and Al are the dominating chemical elements confirming formation of potassium alumina silicates with kaolin addition.

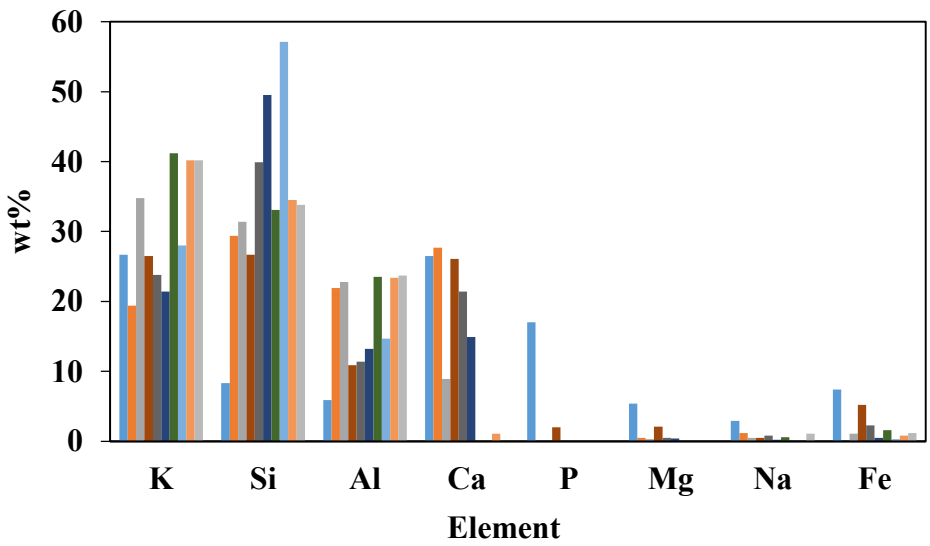

Figure A.5 EDX area analysis of large olive residue + 2% kaolin mixture ash

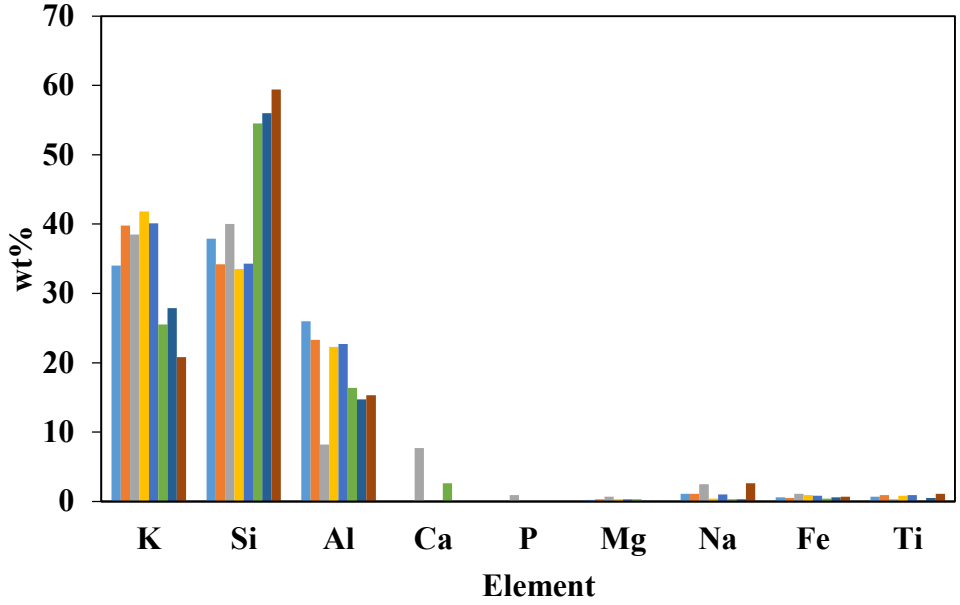

Figure A.6 EDX area analysis of fine olive residue + 2% kaolin mixture ash

SEM images of the overall samples and fine particles in epoxy and a representative SEM image of large and fine olive residue + 8% kaolin mixture ash particles are shown in Figure A.7. As the overall SEM image of samples within the epoxy are investigated, dominance of fine particles is observed indicating reduction of ash sintering tendency of olive residue ash with 8% kaolin addition.

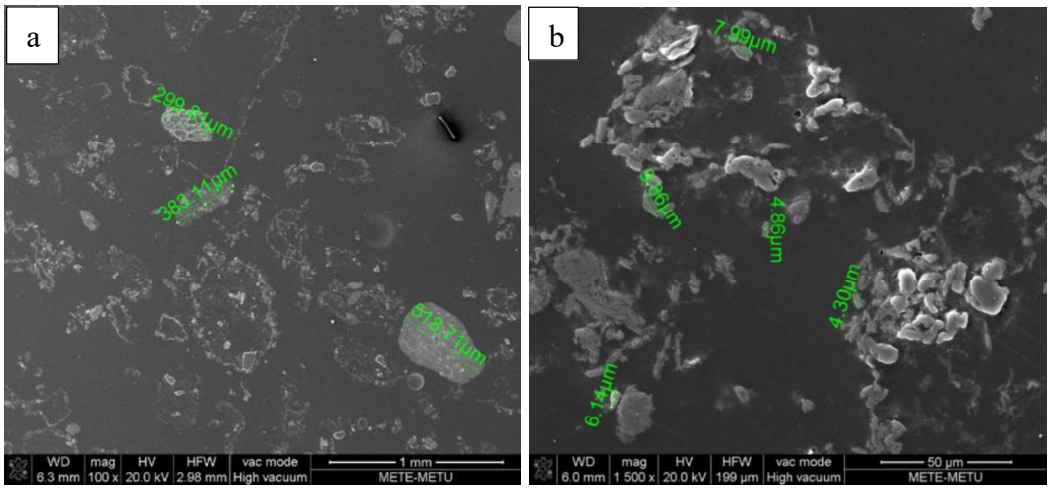

Figure A.7 SEM images of olive residue + 8% kaolin mixture ash (cont'd)

(a: overall image, b: overall fine particles, c: large ash particle, d: fine ash particle)

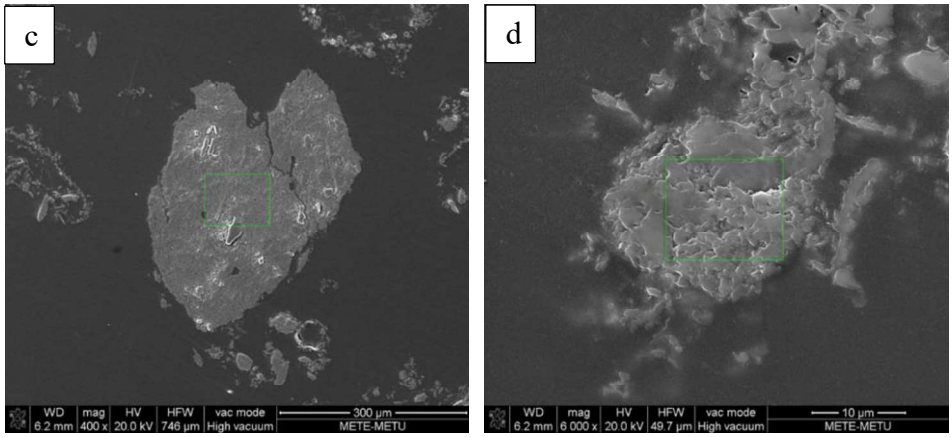

Figure A.7 SEM images of olive residue + 8% kaolin mixture ash

(a: overall image, b: overall fine particles, c: large ash particle, d: fine ash particle)

For large and fine selected ash particles, EDX area analyses were performed and illustrated in Figure A.8 and Figure A.9, respectively. According to EDX area analysis, with 8% kaolin addition, K, Si and Al are observed to be the dominating elements suggesting the formation of high temperature melting potassium aluminum silicates.

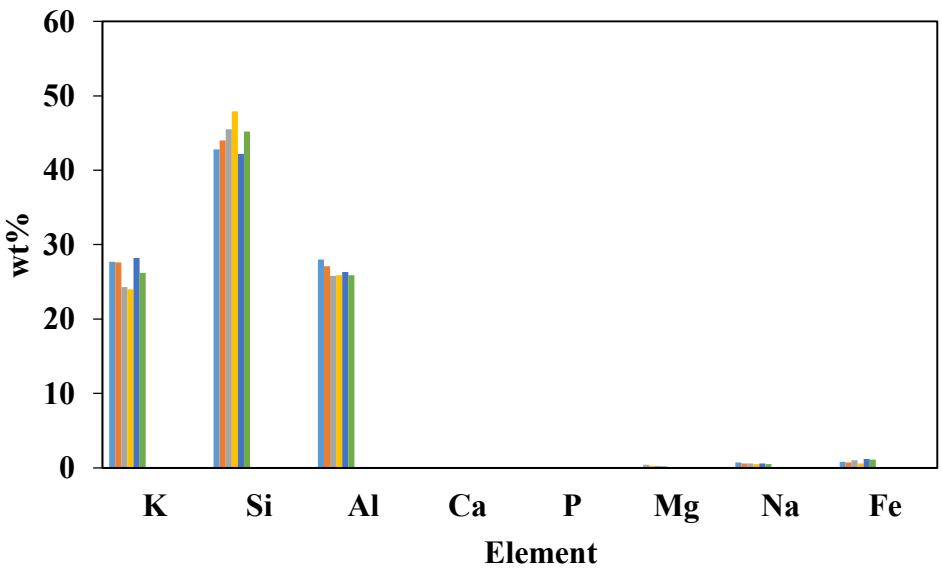

Figure A.8 EDX area analysis of large olive residue + 8% kaolin mixture ash

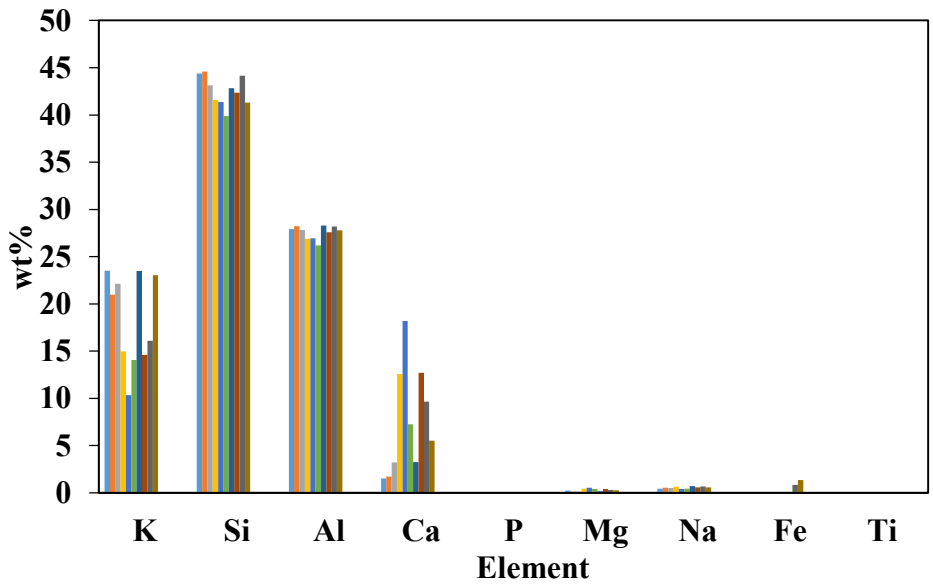

Figure A.9 EDX area analysis of fine olive residue + 8% kaolin mixture ash

In order to observe the effect of kaolin addition on the content of the ash, average of EDX area analysis results are calculated for the ashes of olive residue and olive residue-kaolin mixtures and illustrated in Figure A.10. With increasing kaolin addition, Si and Al content of the ashes increases as expected due to introducing Si and Al elements to the system via kaolin addition.

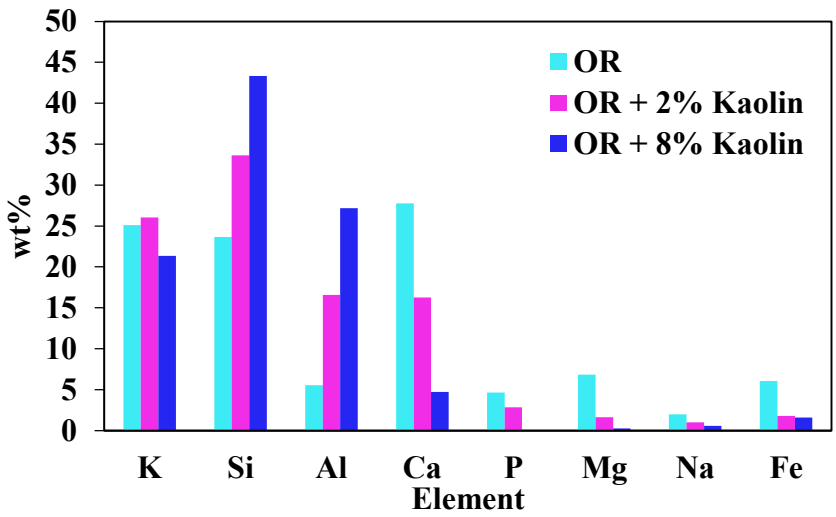

Figure A.10 Average EDX analysis results of ashes of olive residue and olive residue-kaolin mixtures